# Spatial Modulation for Molecular Communication

Yu Huang, Miaowen Wen, *Senior Member, IEEE,* Lie-Liang Yang, *Fellow, IEEE,* Chan-Byoung Chae, *Senior Member, IEEE,* and Fei Ji, *Member, IEEE*

***Abstract*—In this paper, we propose an energy-efficient spatial modulation based molecular communication (SM-MC) scheme, in which a transmitted symbol is composed of two parts, i.e., a space derived symbol and a concentration derived symbol. The space symbol is transmitted by embedding the information into the index of a single activated transmitter nanomachine. The concentration symbol is drawn according to the conventional concentration shift keying (CSK) constellation. Benefiting from a single active transmitter during each symbol period, SM-MC can avoid the inter-link interference problem existing in the current multiple-input multiple-output (MIMO) based MC schemes, which hence enables low-complexity symbol detection and performance improvement. Correspondingly, we propose a low-complexity scheme, which first detects the space symbol by energy comparison, and then detects the concentration symbol by the maximum ratio combining assisted CSK demodulation. In this paper, we analyze the symbol error rate (SER) of the SM-MC and of its special case, namely the space shift keying based MC (SSK-MC), where only space symbol is transmitted and no CSK modulation is invoked. Finally, the analytical results are validated by computer simulations. Our studies demonstrate that both the SSK-MC and SM-MC are capable of achieving better SER performance than the conventional MIMO-MC and single-input single-output based MC, when given the same symbol rate.**

***Index Terms*—Molecular communication, spatial modulation, MIMO, inter-link interference, molecular energy efficiency.**

## I. Introduction

CHEMICAL signalling that exploits molecule or ion for communication has been widely found in nature with diverse propagation distances. In a relatively long range, animals or insects utilize pheromone to communicate with the members of their species for mate selection, identity recognition, alarm inform, etc. [1], [2]. At micro-scale environment, hormones or other chemical substances are prevalently transmitted or received in tiny organisms, such as, cells. This process is the so-called cell signalling, which is crucial to cells' survival [3].

Molecular communication (MC) is an emerging technique inspired from the aforementioned communication schemes in vivo, whose history dates back to 2005 [4]. MC is available at both macro-scale and micro-scale [5]. At micro-scale, MC is suitable for connection among nanomachines, whose communication distance ranges from a nanometer to a hundred nanometers. Nanomachine is one of the most remarkable progress of nanotechnology that has the potential to revolutionize many aspects of technology, and ultimately benefit our life. However, a single nanomachine can only perform very simple tasks due to its size constraint, whereas complex applications including biopsy, targeted drug delivery, environmental sensing, cell sorting, etc., require coordination among a swarm of nanomachines [6]. MC is regarded as a prominent candidate for nanonetworking because of its biocompatible and energy-efficient characteristics. It has been acknowledged as the most important communication paradigm in IEEE 1906.1 standard [7].

### A. Related Work

Modulation plays a significant role in MC as it determines the system's achievable performance [8]. There are a few of modulation schemes for MC proposed in literature, including the concentration shift keying (CSK) [9], molecular shift keying (MoSK) [9], isomer-based ratio shift keying (IRSK) [10] and pulse position modulation (PPM) [11]. Correspondingly, in these modulation schemes, messages are encoded as the concentration, type, ratio and release time of transmitted molecules, respectively. Advanced modulation schemes have also been considered in the context of the single-input single-output based MC (SISO-MC) [12]–[14]. In addition, directionality of the MC transmitters has been considered as the chemical propagation patterns released by transmitter results in different molecular signals, presenting at the receivers at different positions [15], which can be be regarded as a new degree of freedom to convey information in the spatial domain. Such directionality can be provided by the impulsive force at the transmitter as well [16]. Nevertheless, SISO-MC is not always suitable for the scenarios of high-speed transmission and some of the applications where reliability is indispensable. To solve these problems, some well-known techniques in the conventional wireless communications, e.g., multiple-input multiple-output (MIMO), have been redesigned for MC [17]. Specifically, MIMO based MC (MIMO-MC) is a recent trend in MC research, dated back to 2012 when it was first proposed in [18]. It is shown that in MIMO-MC, spatial diversity enhances the bit error rate (BER) performance, while spatial multiplexing may increase transmission rate significantly [18]. In

This work was supported in part by the National Natural Science Foundation of China under Grant 61871190, in part by the Natural Science Foundation of Guangdong Province under Grants 2016A030308006 and 2018B030306005, in part by the Pearl River Nova Program of Guangzhou under Grant 201806010171, and in part by the State Key Laboratory of Integrated Service Networks of Xidian University under Grant ISN20-16. *(Corresponding author: Miaowen Wen.)*

Y. Huang and M. Wen are with the School of Electronics and Information Engineering, South China University of Technology, Guangzhou 510641, China, and also with the State Key Laboratory of Integrated Service Networks, Xidian University, Xi'an 710071, China (e-mail: ee06yuhuang@mail.scut.edu.cn; eemwwen@scut.edu.cn).

L.-L. Yang is with the Southampton Wireless Group, School of Electronics and Computer Science, University of Southampton, Southampton SO17 1BJ, U.K. (e-mail: lly@ecs.soton.ac.uk).

C.-B. Chae is with the Yonsei Institute of Convergence Technology, School of Integrated Technology, Yonsei University, South Korea (e-mail: cbchae@yonsei.ac.kr).

F. Ji are with the School of Electronics and Information Engineering, South China University of Technology, Guangzhou 510641, China (e-mail: eefeiji@scut.edu.cn).

2013, a micro-scale MIMO-MC system was introduced [19], where a group of sender nanomachines simultaneously transmit messages to a group of receiver nanomachines through the medium where they reside. In the same year, the first SISO-MC prototype at macro-scale was implemented [20], which mentioned that MIMO principle may be introduced to improve the transmission rate. In 2016, a $2 \times 2$ MIMO-MC prototype achieving spatial multiplexing was implemented, which achieves a 1.7 times higher data rate than its SISO counterpart [21]. These research and practice demonstrate that spatial multiplexing in MIMO-MC is feasible for rate increase, although the data rate is not doubled due to the existence of interference and overhead. Recently, MIMO-MC techniques have been gaining more attention than ever before. In 2017, a machine learning based channel modeling method [22] and a training-based channel estimation method [23] were proposed for MIMO-MC, respectively. In 2018, the spatial diversity coding techniques, such as the repetition coding and the Alamouti-type coding, were introduced for MIMO-MC in [24]. A blind synchronization was studied in [25] in the context of the single-input multiple-output based MC. Moreover, a MIMO-MC structure with molecular motor as the MC mechanism was investigated in [26]. Now, we have no doubt that MIMO-MC constitutes a promising technique for performance improvement and application extension in MC. However, a typical challenge in MIMO-MC is the inter-link interference (ILI) in addition to the inter-symbol interference (ISI) existing in nearly all MC systems. Due to the ILI, first, the detection complexity at the receiver side is increased. Second, the study in [21] manifests that the BER of a $2 \times 2$ MIMO-MC prototype is 2.2 times higher than that of its SISO-MC counterpart, meaning that high-reliability MIMO-MC is challenging. Third, the energy consumption in MIMO-MC is significant in comparison with that in SISO-MC, due to more devices being simultaneously activated at both transmitter and receiver sides. This problem can be serious in micro-scale MC, since the power supply of nanomachine is limited and their computing capability is low. Consequently, the development of energy-efficient and low-complexity transmission /reception schemes for MIMO-MC is demanding.

Meanwhile, the conventional MIMO technique in wireless communications keeps evolving into a larger scale with numerous antennas, known as massive MIMO. Despite the fact that massive MIMO is able to bring significant improvements in terms of capacity and latency, the challenges with regard to hardware design and signal processing are uncovered [27]. To cope with these challenges, spatial modulation (SM), highly recognized for its low hardware complexity and high energy efficiency, was initially proposed in 2001 as an enhancement of MIMO, whose history of development was fully illustrated in [28]. The principle of SM is to activate one transmit antenna with a specific index to send the corresponding radio signals in each symbol period, whereas other transmit antennas remain idle. Hence, each block of bits in SM is generally divided into two parts, known as the traditional signal constellation, such as PSK/QAM, and the unique spatial constellation, respectively. Without the inter-channel interference (ICI) imposing on SM due to the usage of single transmit antenna, simpler receiver design is possible [28]. SM has formed a wide range of applications, including green wireless networks, distributed wireless networks, visible light communications, etc. [28]. In this paper, we extend the concept of SM further to MIMO-MC.

### B. Our Contributions

We propose an SM based MC (SM-MC) as an alternative for the MIMO-MC implementation, which combines a space-dependent modulation with a concentration-relied modulation. Furthermore, by allowing only the space modulation, we propose the special case of SM-MC, namely, the space shift keying based MC (SSK-MC). It can be shown that both SSK-MC and SM-MC are able to combat the aforementioned problems of the MIMO-MC. It is well known that SM [29] and SSK [30] in radio-based wireless communications exhibit low complexity and high energy efficiency [31]. By exploiting the spatial domain for message encoding via activating an active transmit antenna in each time slot, SM and SSK are also capable of eliminating the ICI. Note that, the major distinction between SM and SSK is that SM uses both spatial and signal constellation to transmit information, while SSK only exploits the spatial constellation.

In our design for SSK-MC, we only consider the spatial domain effect, reflected by the concentration difference presenting at the receiver side, when different transmitters emit molecules. Consequently, non-coherent detection for the space symbol is available in SSK-MC. By contrast, in the design for SM-MC, an extra signal constellation is introduced, which carries information by the different molecular constellation levels in CSK. Hence, in SM-MC, maximum-likelihood (ML) detection is the optimal detection scheme to jointly detect the space and concentration symbols. However, the ML detection for the tiny nanomachine receivers is often prohibitive in practice, as the brute-force search imposes a high complexity. To this end, we propose some low-complexity suboptimal detection schemes for SM-MC systems by detecting the space and concentration symbols separately. In more detail, in these separable detection schemes, firstly, the nanomachine receivers in SM-MC collaborate with each other to identify the activated transmitter nanomachine for detecting the space symbol. Based on the detected space symbol, subsequently, either the selection combining (SC) or the maximal ratio combining (MRC) scheme is developed for detecting the concentration symbol.

In summary, the main contributions of this paper are as follows:

- **Modeling of the SSK-MC/SM-MC:** The SSK-MC and SM-MC schemes are proposed for exploiting the spatial domain degrees of freedom to convey extra information. The novelty of our SM-MC/SSK-MC in contrast to the conventional MIMO-MC [18], [21] is reflected by their capability of eradicating the strongest ILI imposed by the current symbols sent from the unpaired transmitter nanomachine.
- **Design of low-complexity detection schemes for SM-MC:** Instead of the optimal ML detection scheme, we propose some low-complexity suboptimal detection schemes for the SM-MC, which decode the space and

This article has been accepted for publication in a future issue of this journal, but has not been fully edited. Content may change prior to final publication. Citation information: DOI 10.1109/TNB.2019.2905254, IEEE Transactions on NanoBioscience



concentration symbols separately, supported by the various combining strategies proposed.

- **Symbol error rate (SER) analysis for SSK-MC/SM-MC:** Different from the error performance analysis in wireless communications with SM [32], ISI and ILI have to be taken into account in deriving the SER expressions of both the SSK-MC system with non-coherent detection and of the SM-MC system with the MRC-assisted sub-optimal detection. Our analytical results are validated by our simulation results and hence they are beneficial to predict the achievable SER performance of the SSK-MC and SM-MC systems.
- **Performance comparison with existing schemes:** Our performance results show that both SSK-MC and SM-MC significantly outperform the MIMO-MC supporting spatial multiplexing in terms of the SER performance. For some transceiver separation distance, SSK-MC even manifests a better SER performance than the spatial diversity motivated MIMO-MC.

### C. Paper Organization and Notations

The remainder of this paper is organized as follows. Section II reviews the system model of MIMO-MC over diffusion channels. In Section III, we present the principles of SSK-MC and SM-MC based on the architecture of MIMO-MC. In this section, we also derive the SER of the SSK-MC and SM-MC. Section IV evaluates and compares the SER performance of the SSK-MC, SM-MC and other MIMO-MC schemes when various system settings and different transmission/detection schemes are considered. Finally, the research is concluded in Section V.

*Notation*: Boldface uppercase and lowercase letters indicate matrices and vectors, respectively. $\mathbb{R}^{n\times m}$ indicates a real valued matrix with $n \times m$ dimensions. $\mathbb{E}[\cdot]$, $\|\cdot\|$, $|\cdot|$, $Q(\cdot)$ and $\Pr[\cdot]$ represent expectation, Euclidean norm, absolute value, Q-function and probability of an event, respectively.

## II. Review of MIMO-MC

We consider a MIMO-MC system in a 3-D unbounded environment with point transmitter sources and the spherical receivers, which are assumed to be memoryless, and hence without making use of any knowledge of the previously detected symbols. Note that, the memoryless receiver model has typically been considered in literature, such as in [33]–[36], as tiny size nanomachines are anticipated to have low storage space and low computational capability. Perfect synchronization is also assumed in our MIMO-MC. In this section, we propose the channel and communication models for MIMO-MC, which constitutes the fundamentals of our subsequent SM-MC scheme and its special case of the SSK-MC scheme.

### A. Channel Model of MIMO-MC

We consider an $N \times N$ diffusion based MIMO-MC system operated at micro-scale in this paper [19], where $N$ transmit and receive nanomachines are attached to the cell membrane at both transmitter and receiver sides, respectively. Furthermore,

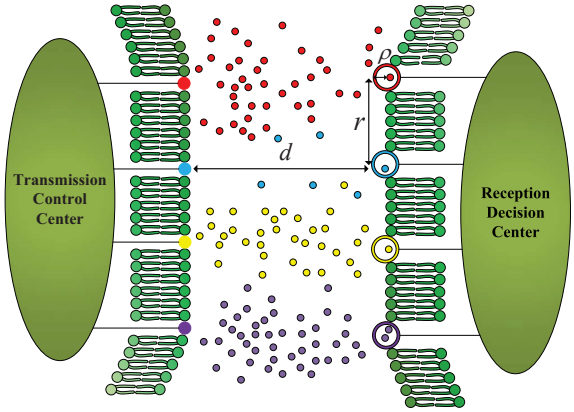


Fig. 1. System model of MIMO-MC.

we assume that there are a transmission control center and a reception decision center, located respectively at the centers of the transmitter and receiver cells. The function of transmission control center is to coordinate the transmitter nanomachines to emit molecular pulses according to the information to be transmitted, while the reception decision center connecting all the receiver nanomachines decodes the information based on the received signals from $N$ receiver nanomachines. To clearly demonstrate the communication system model of the MIMO-MC, we exemplify a $4 \times 4$ MIMO-MC system with 4 pairs of transceivers as shown in Fig. 1, where the lipid bilayer of cell membrane are shown in green color. As shown in Fig. 1, the pair of transmitter and receiver of a link and the molecules transmitted between them are marked using the same color for the sake of easy distinction. Under the assumption that perfect alignment is achieved in the MIMO-MC architecture, the spacing between adjacent transmitters or adjacent receivers is equally set as $r$, and the distance between a pair transmitter and receiver is expressed as $d$. Thus, the distance from the $j$-th transmitter to the $i$-th receiver is given by

$$d_{ji} = \begin{cases} d, & \text{for } i = j, \\ \sqrt{d^2 + |j-i|^2 r^2}, & \text{for } i \neq j. \end{cases} \tag{1}$$

In this paper, we assume $M$-ary CSK modulation and denote the concentration of molecules in the $i$-th receiver at time $t$ in response to the $j$-th transmitter as $c_{m,ij}(t)$ when a pulse of $S_m$ molecules with $m \in \{0, 1, \ldots, M-1\}$ is emitted at $t = 0$. Consequently, the concentration at receiver can be formulated according to Fick's second law of diffusion as [37]

$$c_{m,ij}(t) = S_m \frac{1}{(4\pi D t)^{\frac{3}{2}}} \exp\left(-\frac{d_{ji}^2}{4Dt}\right), \quad \begin{matrix} j \in \{1,2,\ldots,N\}, \\ i \in \{1,2,\ldots,N\}, \\ m \in \{0,1,\ldots,M-1\}, \end{matrix} \tag{2}$$

where $D$ is the diffusion coefficient of the propagation medium that is assumed to be homogeneous in this paper. We assume that the spherical receiver nanomachine has a volume of $V_{\text{RX}} = \frac{4}{3}\pi\rho^3$ with $\rho$ being the radius of the receiver. Molecular concentration is assumed to be uniform inside a passive receiver when $d \gg \rho$. Based on these assumptions, the expected number of molecules inside the $i$-th receiver at

This article has been accepted for publication in a future issue of this journal, but has not been fully edited. Content may change prior to final publication. Citation information: DOI 10.1109/TNB.2019.2905254, IEEE Transactions on NanoBioscience



time $t$ can be given by [38]

$$N_{m,ij}(t) = V_{\mathrm{RX}} c_{m,ij}(t) = V_{\mathrm{RX}} S_m h_{ij}(t), \qquad \text{for } t > 0, \quad (3)$$

where $h_{ij}(t)$ indicates the probability that an information molecule released at $t = 0$ is sensed by the passive receiver at time $t$ [39], which is given by

$$h_{ij}(t) = \frac{1}{(4\pi D t)^{\frac{3}{2}}} \exp\left(-\frac{d_{ji}^2}{4Dt}\right). \quad (4)$$

In MC, $h_{ij}(t)$ represents the channel impulse response (CIR) between the $j$-th transmitter and the $i$-th receiver. Therefore, the concentration vector $\mathbf{c}_{m,j}(t) \in \mathbb{R}^{N\times 1}$ collecting the expected concentration of all receivers in response to the $j$-th transmitter can be written as

$$\begin{aligned}\mathbf{c}_{m,j}(t) &\triangleq \left[c_{m,1j}(t), \ldots, c_{m,ij}(t), \ldots, c_{m,Nj}(t)\right]^T \\ &= S_m \left[h_{1j}(t), \ldots, h_{ij}(t), \ldots, h_{Nj}(t)\right]^T \\ &= S_m \mathbf{h}_j(t), \end{aligned} \quad (5)$$

where $\mathbf{h}_j(t) \in \mathbb{R}^{N\times 1}$ is the CIR vector from the $j$-th transmitter to all the $N$ receivers at time $t$. Let us define $\mathbf{H}(t) \in \mathbb{R}^{N\times N}$ as the channel matrix of an $N \times N$ MIMO-MC system at time $t$, which can be represented as

$$\mathbf{H}(t) = \Big[\mathbf{h}_1(t); \ldots; \mathbf{h}_j(t); \ldots; \mathbf{h}_N(t)\Big], \quad (6)$$

whose entries are given by (4). Based on our assumptions, we can know that the diagonal elements of $\mathbf{H}(t)$, such as $h_{jj}(t)$, have the same value, given by (4) associated with setting $i = j$ and $d_{jj} = d$. By contrast, a non-diagonal element $h_{ij}(t)$ gives the probability of the ILI from the transmitter $j$ to the receiver $i$.

In this paper, we consider the amplitude detection [11]. To achieve this, we assume that all the receivers sense the concentration at a certain time, e.g., at the time when the concentration at a receiver generated by its paired transmitter reaches the peak value, which can be obtained by solving the partial derivative equation $\frac{\partial c_{m,jj}(t)}{\partial t} = 0$. Specifically, when an impulse of molecules is emitted by a transmitter at $t = 0$, the peak concentration presenting at its paired receiver can be found to be at the time of

$$t_p = \frac{d^2}{6D}. \quad (7)$$

Explicitly, the peak time is irrelevant to $S_m$. In this paper, without further explanation, it is assumed that each receiver of the MIMO-MC samples for concentration after a time interval $t_p$ seconds from the emission of the chemical impulse by its paired transmitter. Therefore, upon substituting (1) and (7) into (2), we can derive the maximum concentration of a receiver in response to its paired transmitter as

$$c_{m,jj}(t_p) = S_m \left(\frac{3}{2\pi e d^2}\right)^{\frac{3}{2}}, \quad (8)$$

when an impulse of $S_m$ molecules is released. Similarly, $c_{m,ij}(t_p)$ can be derived, given by

$$c_{m,ij}(t_p) = S_m \left(\frac{3}{2\pi d^2}\right)^{\frac{3}{2}} \exp\left(-\frac{3d_{ji}^2}{2d^2}\right). \quad (9)$$

### B. Communication Model of MIMO-MC

BCSK is the simplest CSK with $M = 2$, which emits a chemical pulse containing $S_1$ molecules towards its paired receiver for transmitting bit "1", or a pulse of $S_0$ molecules for transmitting bit "0". As a special case of BCSK, the OOK modulation, which is prevalently adopted in the existing MIMO-MC [18], [21], [22], [24], keeps silent without any molecule emission for bit "0", i.e., $S_0 = 0$. For the general C-SK, it has been revealed in literature that the CSK with $M \geq 4$ is usually unable to attain satisfactory error performance in SISO-MC [8], [13]. Note that in Fig. 1, we considered OOK as the modulation scheme for MIMO-MC, where the red, yellow, and purple colored links represent transmitting $S_1$ molecules to their corresponding receivers, while the blue colored one keeps silent without any emission of molecules. Furthermore, in Fig. 1, there are still a few of blue-colored molecules, which are the residual molecules of the previous transmissions.

Analogous to the MIMO principles in wireless communications, spatial multiplexing and spatial diversity are two basic operational modes for MIMO-MC. Let us express the transmit signal vector of the MIMO-MC with OOK at the sampling time $t$ as

$$\mathbf{x}(t) = \Big[x_1(t), \ldots, x_i(t), \ldots, x_N(t)\Big]^T, \quad (10)$$

where $x_i(t) \in \{S_0, S_1\}$ denotes the number of molecules emitted by the $i$-th transmitter. Then, based on (6) and (9), the concentration vector corrupted by noise sensed by the receivers at time $t$ can be expressed as

$$\begin{aligned}\mathbf{y}_{\text{MIMO}}(t) &= \Big[y_{1,\,\text{MIMO}}(t), \ldots, y_{i,\,\text{MIMO}}(t), \ldots, y_{N,\,\text{MIMO}}(t)\Big]^T \\ &= \sum_{l=0}^{L} \mathbf{H}(t + lT_s)\mathbf{x}(t - lT_s) + \mathbf{n}_{\text{MIMO}}(t), \end{aligned} \quad (11)$$

where $T_s$ denotes the symbol duration and $y_{i,\,\text{MIMO}}(t)$ represents the concentration sensed by the $i$-th receiver at time $t$. To be consistent with the common representations [23], [24], we also have an analogous form of:

$$y_{i,\,\text{MIMO}}(t) = \sum_{j=1}^{N}\sum_{l=0}^{L} h_{ij}(t + lT_s)x_j(t - lT_s) + n_{i,\,\text{MIMO}}(t), \quad (12)$$

from which we can know that the ISI and ILI last for $L$ and $L + 1$ symbol durations, respectively. This assumption is valid, when the ISI and ILI resulted from the $L$ previously transmitted symbols have a comparable effect in confusing the signal detection. Based on this assumption, it can be inferred that the ILI length is the ISI length plus one, as ILI also comes from the current symbol duration, while ISI is only caused by the previously transmitted symbols from the paired transmitter. The noise vector of MIMO-MC $\mathbf{n}_{\text{MIMO}}(t) \in \mathbb{R}^{N\times 1}$ in (11) can be expressed as

$$\mathbf{n}_{\text{MIMO}}(t) = [n_{1,\,\text{MIMO}}(t), \ldots, n_{i,\,\text{MIMO}}(t), \ldots, n_{N,\,\text{MIMO}}(t)]^T, \quad (13)$$

where $n_{i,\,\text{MIMO}}(t)$, as shown in (12), is a signal dependent noise sensed by the $i$-th receiver. It can be shown that (12) can be

This article has been accepted for publication in a future issue of this journal, but has not been fully edited. Content may change prior to final publication. Citation information: DOI 10.1109/TNB.2019.2905254, IEEE Transactions on NanoBioscience



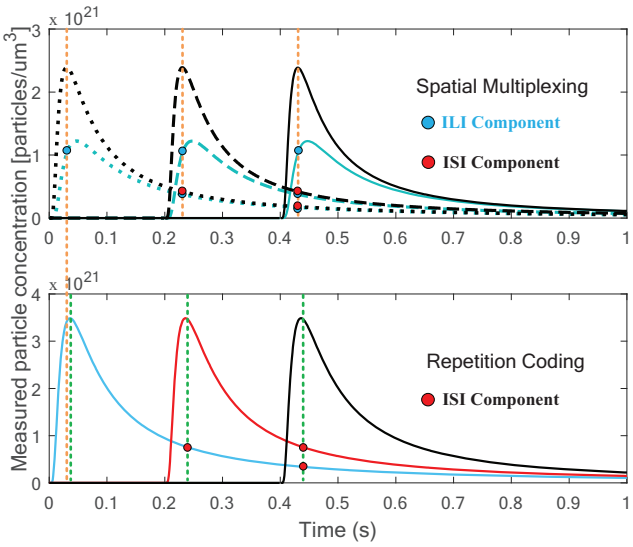


Fig. 2. Concentration expected at one receiver of a $2 \times 2$ MIMO-MC under spatial multiplexing and repetition coding modes affected by its ISI and the ILI from one other link, when SNR $=$ 10 dB, $D = 2.2 \times 10^{-9} m^2/s$, $\rho = 0.1\mu m$, $d = 20\mu m$, $r = 15\mu m$ and $T_s = 0.2s$.

rewritten as

$$y_{i,\,\text{MIMO}}(t) = \underbrace{h_{ii}(t)x_i(t)}_{\text{desired signal}} + \underbrace{I_{i,\,\text{MIMO}}(t)}_{\text{sum of interference}} + \underbrace{n_{i,\,\text{MIMO}}(t)}_{\text{noise}}, \quad (14)$$

where the noise component is assumed to follow the Gaussian distribution, represented as [40]:

$$n_{i,\,\text{MIMO}}(t) \sim \mathcal{N}\big(\mu_{ni,\,\text{MIMO}}(t), \sigma^2_{ni,\,\text{SM}}(t)\big), \quad (15)$$

associated with

$$\mu_{ni,\,\text{MIMO}}(t) = 0, \quad \sigma^2_{ni,\,\text{SM}}(t) = \frac{h_{ii}(t)x_i(t) + I_{i,\,\text{MIMO}}(t)}{V_{\text{RX}}}.$$

The impact of ISI and ILI on the desired signal presenting in a receiver nanomachine is illustrated in Fig. 2, where a $2 \times 2$ MIMO-MC system under the modes of spatial multiplexing and repetition coding is assumed to transmit a three-consecutive-signals vector $[S_1, S_1, S_1]$ by each of the nanomachine transmitters. In this case, the receiver nanomachines are symmetrical, as indicated in [24]. Hence, we can simply consider a received molecular signal in an arbitrary nanomachine receiver. As shown in Fig. 2, the ILI is not only generated from the previous molecular symbols, but mostly generated from the current one released by the unpaired transmitter. Hence, the current ILI plays the most significant role in confusing the detection of a desired molecular signal. From the effect of ISI, the existing studies on SISO-MC usually only take one previous symbol into account, ignoring the ISI from the further previous symbols [9], [41], [42], due to the fact that the symbol preceding the current symbol dominates the ISI. Additionally, as shown in Fig. 2, the effect of the current ILI may significantly surpass that of the ISI. From above analysis we can infer that the interference in the MIMO-MC systems under spatial multiplexing mode is usually dominated by the current ILI generated by the other unpaired transmitters, and

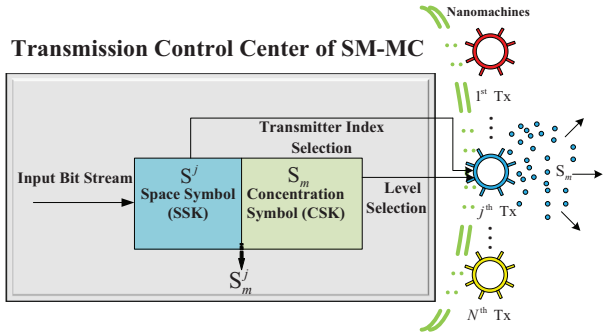


Fig. 3. Transmitter diagram of SM-MC.

by the ISI generated by one previous symbol transmitted by the paired transmitter. By contrast, in the MIMO-MC systems employing repetition coding, the ILI has a constructive effect for signal detection, as it enhances the desired signals' strength [24] at the expense of transmission rate. Based on the above analysis, we approximate the interference component in (14) as

$$I_{i,\,\text{MIMO}}(t) \approx \underbrace{\sum\nolimits_{j \neq i} h_{ij}(t)x_j(t)}_{\text{current ILI}} + \underbrace{h_{ii}(t+T_s)x_i(t-T_s)}_{\text{last ISI}}. \quad (16)$$

## III. Spatial Modulation Based Molecular Communication

From the above description, we can know that MIMO-MC experiences both ILI and ISI, which may significantly degrade the detection performance. In order to combat these problems, in this section, we propose the SM-MC as one of the implementation of the MIMO-MC. In our proposed scheme, both spatial and concentration domains are exploited for conveying information simultaneously, but only one type of molecules is used for transmission.

The ideology of SM-MC is inspired by the SSK technique having been widely studied in MIMO communications. Typically, in SSK modulation, only one transmit antenna is activated during each symbol period. At the receiver, the index of the activated transmit antenna can be detected, when the channel state information is available. The SSK modulation can be implemented in conjunction with a conventional amplitude-phase modulation, forming the SM [28]. Similarly, the SM-MC proposed in this paper is the combination of a SSK modulation and a CSK modulation. Specifically, given a symbol transmitted, one of the transmitter nanomachines releases a pulse of molecules, with the number of molecules determined also by the data symbol being transmitted. In detail, the transmit schematic diagram for our SM-MC system is depicted in Fig. 3. Hence, when the $j$-th space symbol is transmitted, with $j \in \{1, 2, \ldots, N\}$, the transmit signal vector has a form of

$$\mathbf{x}(t) = \Big[0, 0, \ldots, \underbrace{S_m}_{\text{j-th transmitter}}, \ldots, 0, 0\Big]^T, \quad (17)$$

where only the $j$-th transmitter is activated to emit $S_m > 0$ molecules, when the $m$-th concentration symbol $S_m$ is selected. The space symbol is denoted as $S^j$, when the $j$-th

This article has been accepted for publication in a future issue of this journal, but has not been fully edited. Content may change prior to final publication. Citation information: DOI 10.1109/TNB.2019.2905254, IEEE Transactions on NanoBioscience



transmitter is activated. We assume that the space symbols $S^j$ and the concentration symbols $S_m$ are independent of each other, solely depended on the input data stream. Then, we have

$$\Pr[S_m] = \frac{1}{M}, \quad m \in \{0, 1, \ldots, M-1\}, \tag{18}$$

and

$$\Pr[S^j] = \frac{1}{N}, \quad j \in \{1, 2, \ldots, N\}. \tag{19}$$

### A. Transmitter of SM-MC

Furthermore, if we express the SM symbols representing the combinations of the space and concentration symbols as $S_m^j$, we have

$$\Pr[S_m^j] = \frac{1}{MN}, \begin{array}{c} j \in \{1, 2, \ldots, N\}, \\ m \in \{0, 1, \ldots, M-1\}. \end{array} \tag{20}$$

Therefore, the raw data rate of the SM-MC measured in *bits per molecular symbol* is given as

$$R_{\text{SM}} = \log_2 N + \log_2 M, \tag{21}$$

where both the values of $N$ and $M$ are assumed to be an integer power of 2.

Based on (17), the concentration signal observed at the $i$-th receiver in the SM-MC systems is similar to (14), expressed as

$$y_{i,\,\text{SM}}(t) = S_m h_{ij}(t) + I_{i,\,\text{SM}}(t) + n_{i,\,\text{SM}}(t), \tag{22}$$

where both $S_m h_{ij}(t)$ and $n_{i,\,\text{SM}}(t)$ are dependent on the current molecular symbol being received, representing the expected number of molecules received and the noise component, respectively, at time $t$, when the $j$-th transmitter is activated to emit a chemical impulse with $S_m$ molecules. However, unlike the case in MIMO-MC [21], the $I_{i,\,\text{SM}}(t)$ in (22) consists of only the ISI component that is resulted from a previous molecular symbol emitted by the $i$-th transmitter, since we assume that ILI only occurs with the current transmission, while ISI is only experienced from one previous emission by a paired transmitter. Let us denote the previous molecular symbol as $S_{\bar{m}}^{\bar{j}}$, then we have

$$I_{i,\,\text{SM}}(t) = \begin{cases} 0, & \text{for } i \neq j, \\ S_{\bar{m}} h_{ii}(t + T_s), & \text{for } i = \bar{j}. \end{cases} \tag{23}$$

Similar to (15), the distribution of the noise component in (22) can be expressed as

$$n_{i,\,\text{SM}}(t) \sim \mathcal{N}\Big(\mu_{ni,\,\text{SM}}(t), \sigma^2_{ni,\,\text{SM}}(t)\Big), \tag{24}$$

associated with

$$\mu_{ni,\,\text{SM}}(t) = 0, \quad \sigma^2_{ni,\,\text{SM}}(t) = \frac{S_m h_{ij}(t) + I_{i,\,\text{SM}}(t)}{V_{\text{RX}}}.$$

Furthermore, based on (22), (23) and (24), the distribution of $y_{i,\,\text{SM}}(t)$ can be found, and expressed as

$$y_{i,\,\text{SM}}(t) \sim \mathcal{N}\Big(S_m h_{ij}(t) + I_{i,\,\text{SM}}(t), \sigma^2_{ni,\,\text{SM}}(t)\Big). \tag{25}$$

TABLE I
IDEAL DATA RATE FOR DIFFERENT MODULATION SCHEMES IN MC

| Scheme | Ideal data rate | Scheme | Ideal data rate |
|---|---|---|---|
| OOK | 1 | BCSK | 1 |
| BMoSK | 1 | BSSK | 1 |
| $2 \times 2$ MIMO (OOK) | 2 | QCSK | 2 |
| $2 \times 2$ SM (BCSK) | 2 | QSSK | 2 |
| $4 \times 4$ SM (BCSK) | 3 | 8SSK | 3 |
| $2 \times 2$ SM (QCSK) | 3 | 16SSK | 4 |

Corresponding to (11), the concentration vector sensed at the $N$ receivers in the SM-MC system is expressed as

$$\mathbf{y}_{\text{SM}}(t) = \Big[y_{1,\,\text{SM}}(t), \ldots, y_{i,\,\text{SM}}(t), \ldots, y_{N,\,\text{SM}}(t)\Big]^T. \tag{26}$$

From the above analysis and (23), we can readily realize that our proposed SM-MC transmission scheme is capable of getting rid of the most significant ILI generated by the signals sent by the unpaired transmitters during the current symbol period, which is unavoidable in the general MIMO-MC [18], [21]. Furthermore, the ILI generated by the previous symbols can also be significantly mitigated owning to the employment of the SSK modulation. In addition to the benefit of ILI mitigation, the SSK-MC and SM-MC schemes are more energy efficient than the conventional MIMO-MC, which to the best of our knowledge, has not been quantified in terms of BER in literature. Note that the energy efficiency of the MC systems has been considered in [13], where only the number of molecules for transmitting a bit is concerned, regardless of the data rate. By contrast, in this paper, we define the molecular energy efficiency is defined as

$$\eta = \frac{R(1 - P_e)}{\bar{S}} \approx \frac{\bar{R}}{\bar{S}}, \tag{27}$$

whose unit is *bits per molecule*. This definition corresponds to the concept of energy efficiency in wireless communications [43], measured in *bits per Joule*. In (27), $P_e$ is the BER, $\bar{S}$ is the mean number of molecules released for each transmission, $R$ is the raw data rate given in (21) and $\bar{R}$ is the achievable rate. Simulation results in Section IV demonstrate that the SSK-MC and SM-MC schemes are capable of attaining lower $P_e$ than the conventional MIMO-MC under the same $R$ and $\bar{S}$. Hence, according to [28], SSK-MC and SM-MC are capable to obtain higher molecular energy efficiency than the conventional MIMO-MC. For convenience, the raw data rates $R$ of some modulation techniques for MC are illustrated in Table I.

The reason behind the above results can be interpreted in detail as follows. For an $N \times N$ MIMO-MC with a fixed modulation scheme, increasing $N$ may achieve a higher raw data rate but at the expense of the degraded error performance. This is because first, the number of molecules released per transmitter is $\bar{S}/N$, which reduces as $N$ increases. Second, a larger $N$ infers that ILI is imposed by more undesired links, which further degrades the error performance. By contrast, for the SM-MC and its special scheme of SSK-MC, owing to their capability of ILI mitigation, they can obtain a raw data rate of logarithmically increasing. This is solely contributed by the space domain degrees of freedom without demanding any extra

transmission energy (molecules) and introducing additional ILI. Therefore, we may argue that the SSK-MC and SM-MC schemes are suitable for the micro-scale communication scenarios, where energy supply is limited.

### *B. Signal Detection in SM-MC Systems*

In theory, the ML detection achieving optimal detection performance can be implemented with the SM-MC in order to jointly decode the space and concentration symbols. When memoryless receivers are considered, the optimal ML detection based on (22) and (26) can be formulated as

$$< \hat{j}, \hat{m} >= \underset{j\in\{1,2,\ldots,N\}, m\in\{0,1,\ldots,M-1\}}{\arg\min} \left\|\mathbf{y}_{\text{SM}}(t) - S_m \mathbf{h}_j(t)\right\|^2, \tag{28}$$

where $\hat{j}$ and $\hat{m}$ are the estimated indices of the space and concentration symbols, respectively. Note that $S_m$ in SM-MC is always greater than zero, i.e., $S_m > 0$, otherwise the space symbols in the case of $S_m = 0$ are unable to be detected. Eq. (28) infers that the ML detector has a search complexity of $\mathcal{O}(NM)$. Explicitly, when $NM$ is relatively large, it is not practical to be deployed with MC systems, owing to the constraint on the size and computing capability of MC receivers. Therefore, low complexity detection schemes are desirable for MC. In wireless communications, a range of suboptimal detectors have been proposed for SM to reduce the detection complexity [44]–[47]. However, these suboptimal detectors in general cannot be directly adopted for MIMO-MC systems due to the fact that the channel matrix in SM-MC is real and non-negative [24], which is different from that in wireless communications, where the channel matrix is complex. Besides, because of the slow propagation velocity of molecules, MC usually suffers from severe ISI and ILI, which also prevents from directly employing the suboptimal detectors proposed for the SM in wireless communications. To this end, we below propose a low-complexity successive detection scheme for the SM-MC. In this scheme, the CSK symbol is detected after the detection of the space symbol as follows. First, to be more specific, the index of the activated transmitter is detected via comparison of the concentration sensed by the $N$ receivers, based on the fact that the receiver paired with the activated transmitter is most likely to have the maximum concentration at the sampling time, because it is located with the minimum distance from its paired active transmitter. This is a non-coherent detection scheme, which can be formulated as

$$\hat{j} = \underset{j\in\{1,2,\ldots,N\}}{\arg\max}\ y_{j,\,\text{SM}}(t). \tag{29}$$

After the detection of the space symbol, the concentration observed by all the $N$ receivers can be exploited for detecting the CSK symbol, which can be formulated as:

$$\hat{m}= \underset{m\in\{0,1,\ldots,M-1\}}{\arg\min} \left\|\mathbf{w}^T\mathbf{y}_{\text{SM}}(t) - S_m \mathbf{w}^T\mathbf{h}_{\hat{j}}(t)\right\|^2, \tag{30}$$

where $\mathbf{w}\in\mathbb{R}^{N\times 1}$ is a weighting vector of length-$N$, expressed as

$$\mathbf{w} = [w_1, \ldots, w_i, \ldots, w_N]^T, \tag{31}$$

which may be different when different combining strategies are employed. In this paper, we propose and investigate two types of combining strategies that are commonly used in wireless communications, which are selection combining (SC) and maximal ratio combining (MRC). Specifically, when the SC-assisted detector is employed, only the $\hat{j}$-th receiver's concentration, where $\hat{j}$ is obtained from the space symbol detection, as seen in (29), is utilized to detect the concentration symbol. In this case, the components in (31) are given the values as

$$w_i = \begin{cases} 1, & \text{for } i = \hat{j}, \\ 0, & \text{otherwise.} \end{cases} \tag{32}$$

Then, upon applying these results into (30), the CSK symbol index detected using the SC-assisted detection can be described as

$$\begin{aligned}
\hat{m}_{\text{SC}} &= \underset{m\in\{0,1,\ldots,M-1\}}{\arg\min} \left| y_{\hat{j},\,\text{SM}}(t) - S_m h_{\hat{j}\hat{j}}(t)\right|^2 \\
&= \underset{m\in\{0,1,\ldots,M-1\}}{\arg\min} y^2_{\hat{j},\,\text{SM}}(t) - 2S_m y_{\hat{j},\,\text{SM}}(t) h_{\hat{j}\hat{j}}(t) + \left(S_m h_{\hat{j}\hat{j}}(t)\right)^2 \\
&\overset{(a)}{=} \underset{m\in\{0,1,\ldots,M-1\}}{\arg\min} \left(S_m h_{\hat{j}\hat{j}}(t)\right)^2 - 2S_m y_{\hat{j},\,\text{SM}}(t) h_{\hat{j}\hat{j}}(t) \\
&\overset{(b)}{=} \underset{m\in\{0,1,\ldots,M-1\}}{\arg\min} \left(S_m\right)^2 h_{\hat{j}\hat{j}}(t) - 2S_m y_{\hat{j},\,\text{SM}}(t),
\end{aligned} \tag{33}$$

where from (a) to (b) is due to $h_{\hat{j}\hat{j}}(t)$ being a real positive number. From (33), we can readily know that the complexity of our proposed SC-assisted detector is $\mathcal{O}(N+M)$. Provided that $N > 2$ or $M > 2$, the complexity of the SC-assisted detector is lower than that of the optimal ML detector of (28).

When the MRC detector is employed, we have $\mathbf{w} = \mathbf{h}_{\hat{j}}(t)$. Correspondingly, the CSK symbol index can be estimated from the optimization problem of

$$\begin{aligned}
\hat{m}_{\text{MRC}} &= \underset{m\in\{0,1,\ldots,M-1\}}{\arg\min} \left|\mathbf{h}^T_{\hat{j}}(t)\mathbf{y}_{\text{SM}}(t) - S_m \|\mathbf{h}_{\hat{j}}(t)\|^2\right|^2 \\
&= \underset{m\in\{0,1,\ldots,M-1\}}{\arg\min} \|\mathbf{h}^T_{\hat{j}}(t)\mathbf{y}_{\text{SM}}(t)\|^2 - 2S_m \mathbf{h}^T_{\hat{j}}(t)\mathbf{y}_{\text{SM}}(t)\|\mathbf{h}_{\hat{j}}(t)\|^2 \\
&\qquad + (S_m)^2 \|\mathbf{h}_{\hat{j}}(t)\|^4 \\
&= \underset{m\in\{0,1,\ldots,M-1\}}{\arg\min} \|\mathbf{h}_{\hat{j}}(t)\|^2 \left[(S_m)^2\|\mathbf{h}_{\hat{j}}(t)\|^2 - 2S_m \mathbf{h}^T_{\hat{j}}(t)\mathbf{y}_{\text{SM}}(t)\right] \\
&= \underset{m\in\{0,1,\ldots,M-1\}}{\arg\min} (S_m)^2\|\mathbf{h}_{\hat{j}}(t)\|^2 - 2S_m \mathbf{h}^T_{\hat{j}}(t)\mathbf{y}_{\text{SM}}(t).
\end{aligned} \tag{34}$$

Alternatively, after the space symbol is detected, if we use the ML detection to detect the CSK symbol, the detection problem can be described as

$$\begin{aligned}
\hat{m}_{\text{Sub-ML}} &= \underset{m\in\{0,1,\ldots,M-1\}}{\arg\min} \left\|\mathbf{y}_{\text{SM}}(t) - S_m \mathbf{h}_{\hat{j}}(t)\right\|^2 \\
&= \underset{m\in\{0,1,\ldots,M-1\}}{\arg\min} \|\mathbf{y}_{\text{SM}}(t)\|^2 - 2S_m \mathbf{y}^T_{\text{SM}}(t)\mathbf{h}_{\hat{j}}(t) + (S_m)^2\|\mathbf{h}_{\hat{j}}(t)\|^2 \\
&= \underset{m\in\{0,1,\ldots,M-1\}}{\arg\min} (S_m)^2\|\mathbf{h}_{\hat{j}}(t)\|^2 - 2S_m \mathbf{y}^T_{\text{SM}}(t)\mathbf{h}_{\hat{j}}(t).
\end{aligned} \tag{35}$$

Intuitively, we have $\mathbf{y}^T_{\text{SM}}(t)\mathbf{h}_{\hat{j}}(t) = \mathbf{h}^T_{\hat{j}}(t)\mathbf{y}_{\text{SM}}(t)$. Hence the detection problem of (34) is the same as that of (35), meaning

This article has been accepted for publication in a future issue of this journal, but has not been fully edited. Content may change prior to final publication. Citation information: DOI 10.1109/TNB.2019.2905254, IEEE Transactions on NanoBioscience



that the MRC-assisted detector is equivalent to the ML detector for detecting the CSK symbol, and hence the MRC-assisted detection is also optimum.

From (34) we can obtain the complexity of the MRC-assisted detector is also $\mathcal{O}(N+M)$, although the total number of computation of (34) is significantly higher than that of (33). As shown by our simulation results in Section IV, the error performance of the MRC-assisted detector may significantly outperform that of the SC-assisted detector.

### C. Error Performance Analysis of SM-MC

In this subsection, we focus on the SER analysis of the MRC-assisted detection, given by (29) and (34). Since the detection is dependent on both the current molecular symbol $S_m^j$ and one previous symbol $S_{\bar{m}}^{\bar{j}}$, let us denote the correct detection probability of the space and concentration symbols as $P_{c,\,\text{SSK}}(S_m^j|S_{\bar{m}}^{\bar{j}})$ and $P_{c,\,\text{CSK}}(S_m^j|S_{\bar{m}}^{\bar{j}})$, respectively. Remembering that $S_m^j$ and $S_{\bar{m}}^{\bar{j}}$ are mutually independent, we can express the correct detection probability of the space symbol as

$$P_{c,\,\text{SSK}}(S_m^j|S_{\bar{m}}^{\bar{j}}) = \prod_{i\neq j} Q\left(-\frac{\mu_{ji|S_{\bar{m}}^{\bar{j}}}}{\sigma_{ji|S_{\bar{m}}^{\bar{j}}}}\right), \tag{36}$$

where $Q(\cdot)$ is the Q-function. When given $i \neq j$, $\mu_{ji|S_{\bar{m}}^{\bar{j}}}$ and $\sigma^2_{ji|S_{\bar{m}}^{\bar{j}}}$ can be shown to be

$$\mu_{ji|S_{\bar{m}}^{\bar{j}}} = \begin{cases} S_m\big(h_{jj}(t)-h_{ij}(t)\big)-S_{\bar{m}}h_{ii}(t+T_s), & \text{for } i=\bar{j} \text{ and } j\neq\bar{j}, \\ S_m\big(h_{jj}(t)-h_{ij}(t)\big)+S_{\bar{m}}h_{jj}(t+T_s), & \text{for } i\neq\bar{j} \text{ and } j=\bar{j}, \\ S_m\big(h_{jj}(t)-h_{ij}(t)\big), & \text{for } i\neq\bar{j} \text{ and } j\neq\bar{j}. \end{cases}$$

$$\sigma^2_{ji|S_{\bar{m}}^{\bar{j}}} = \begin{cases} \frac{S_m\left(h_{jj}(t)+h_{ij}(t)\right)+S_{\bar{m}}h_{ii}(t+T_s)}{V_{\text{RX}}}, & \text{for } i=\bar{j} \text{ and } j\neq\bar{j}, \\ \frac{S_m\left(h_{jj}(t)+h_{ij}(t)\right)+S_{\bar{m}}h_{jj}(t+T_s)}{V_{\text{RX}}}, & \text{for } i\neq\bar{j} \text{ and } j=\bar{j}, \\ \frac{S_m\left(h_{jj}(t)+h_{ij}(t)\right)}{V_{\text{RX}}}, & \text{for } i\neq\bar{j} \text{ and } j\neq\bar{j}. \end{cases}$$

*Proof:* See Appendix A. ■

Specifically, when only the space symbol $S^j$ is transmitted, meaning that $M = 1$, the SM-MC degenerates to the SSK-MC. Correspondingly, the non-coherent detection of (29) can be implemented. In this case, the detection performance of the SSK-MC can be derived first finding the probability of $P_{c,\,\text{SSK}}(S^j|S^{\bar{j}})$, where $S^j$ and $S^{\bar{j}}$ are mutually independent, and both of them are positive numbers. Consequently, when considering that the transmitted symbols are uniformly distributed, the average correct detection probability can be derived as

$$\begin{aligned} P_{c,\,\text{SSK}} &= \mathbb{E}\Big[\mathbb{E}\big[P_{c,\,\text{SSK}}(S^j|S^{\bar{j}})\big]\Big] \\ &= \sum_{j=1}^{N}\sum_{\bar{j}=1}^{N} P_{c,\,\text{SSK}}(S^j|S^{\bar{j}})\text{Pr}[S^{\bar{j}}]\text{Pr}[S^j] \\ &= \frac{1}{N^2}\sum_{j=1}^{N}\sum_{\bar{j}=1}^{N}\prod_{i\neq j} Q\left(\frac{-\mu_{ji|S^{\bar{j}}}}{\sigma_{ji|S^{\bar{j}}}}\right), \end{aligned} \tag{37}$$

where the inner $\mathbb{E}$ is with respect to the one previous symbol, while the outer $\mathbb{E}$ is in terms of the current symbol. Correspondingly, the SER of the SSK-MC is given by

$$P_{e,\,\text{SSK}} = 1 - P_{c,\,\text{SSK}} = 1 - \frac{1}{N^2}\sum_{j=1}^{N}\sum_{\bar{j}=1}^{N}\prod_{i\neq j} Q\left(\frac{-\mu_{ji|S^{\bar{j}}}}{\sigma_{ji|S^{\bar{j}}}}\right). \tag{38}$$

Having considered the space symbol, the error rate of the CSK detection can be analyzed based on the estimate $\hat{j}$. Here, we analyze the MRC-assisted detector of (34) due to its low complexity and optimum SER performance for detection of the concentration symbol. In order to carry out the analysis, let us assume that a pulse of $S_m$ molecules is transmitted by the $j$-th transmitter and that the previously emitted molecular symbol is $S_{\bar{m}}^{\bar{j}}$. Then, the probability of erroneous detection of the CSK symbol can be upper bounded by

$$P_{e,\,\text{CSK}}(S_m^j|S_{\bar{m}}^{\bar{j}}) \leqslant \sum_{m\neq n}\text{Pr}[S_m \to S_n|S_{\bar{m}}^{\bar{j}}], \tag{39}$$

where $\text{Pr}[S_m \to S_n|S_{\bar{m}}^{\bar{j}}]$ is also dependent on the detection of the space symbol, which can be expressed as

$$\begin{aligned} \text{Pr}[S_m \to S_n|S_{\bar{m}}^{\bar{j}}] = &\sum_{\hat{j}\neq j}\text{Pr}_{\,\text{SSK}}[\hat{j}|S_{\bar{m}}^{\bar{j}}]\ \text{Pr}[S_m \to S_n|S_{\bar{m}}^{\bar{j}},\hat{j}] \\ &+ \text{Pr}_{\,\text{SSK}}[j|S_{\bar{m}}^{\bar{j}}]\ \text{Pr}[S_m \to S_n|S_{\bar{m}}^{\bar{j}},j], \end{aligned} \tag{40}$$

where $\text{Pr}_{\,\text{SSK}}[\hat{j}|S_{\bar{m}}^{\bar{j}}]$ and $\text{Pr}_{\,\text{SSK}}[j|S_{\bar{m}}^{\bar{j}}]$ have been derived in (48) of Appendix A for the detection of the SSK symbol. Hence, below we only need to focus on the unknown components, i.e., $\text{Pr}[S_m \to S_n|S_{\bar{m}}^{\bar{j}},\hat{j}]$ and $\text{Pr}[S_m \to S_n|S_{\bar{m}}^{\bar{j}},j]$, in (40), which are given by (41) and (42), respectively, shown on the top of the next page. In these formulas, the $\sigma^2_{ni,\,\text{SM}}(t)$ component has been defined in (24).

Consequently, when both the SSK and the CSK symbols are considered, the error probability of the SM-MC system conditioned on that $S_m^j$ and $S_{\bar{m}}^{\bar{j}}$ are transmitted as the current and previous symbol, is given by

$$\begin{aligned} P_{e,\,\text{SM}}(S_m^j|S_{\bar{m}}^{\bar{j}}) =& 1-\Big(1-P_{e,\,\text{SSK}}(S_m^j|S_{\bar{m}}^{\bar{j}})\Big)\Big(1-P_{e,\,\text{CSK}}(S_m^j|S_{\bar{m}}^{\bar{j}})\Big) \\ \leqslant& P_{e,\,\text{SSK}}(S_m^j|S_{\bar{m}}^{\bar{j}}) + \sum_{m\neq n}\text{Pr}[S_m \to S_n|S_{\bar{m}}^{\bar{j}}] \\ &- P_{e,\,\text{SSK}}(S_m^j|S_{\bar{m}}^{\bar{j}})\sum_{m\neq n}\text{Pr}[S_m \to S_n|S_{\bar{m}}^{\bar{j}}]. \end{aligned} \tag{43}$$

Furthermore, if we ignore the negative term in (43), we have

$$P_{e,\,\text{SM}}(S_m^j|S_{\bar{m}}^{\bar{j}}) \leqslant P_{e,\,\text{SSK}}(S_m^j|S_{\bar{m}}^{\bar{j}}) + \sum_{m\neq n}\text{Pr}[S_m \to S_n|S_{\bar{m}}^{\bar{j}}]. \tag{44}$$

When comparing (43) and (44), we can see that when the signal-to-noise ratio (SNR) is sufficiently high, making the detection of both the SSK and CSK symbols sufficiently reliable, we can ignore the production term in (43), and directly use (44) to obtain the approximate conditional error probability, as shown in Section IV.

$$\Pr[S_m \to S_n|S_{\bar{m}}^{\bar{j}}, \hat{j}] = \Pr\left[\sum_{i=1}^{N}|y_{i,\,\mathrm{SM}}(t) - S_m h_{i\hat{j}}(t)|^2 > \sum_{i=1}^{N}|y_{i,\,\mathrm{SM}}(t) - S_n h_{i\hat{j}}(t)|^2 \Big| S_{\bar{m}}^{\bar{j}}\right]$$
$$= \begin{cases} 1 - Q\left(\frac{-S_{\bar{m}}h_{\bar{j}\hat{j}}(t)h_{\bar{j}j}(t+T_s) - S_m\sum_{i=1}^{N}h_{i\hat{j}}(t)h_{ij}(t) + \frac{(S_m+S_n)}{2}\sum_{i=1}^{N}h_{i\hat{j}}^2(t)}{\sqrt{\sum_{i=1}^{N}h_{i\hat{j}}^2(t)\sigma_{ni,\,\mathrm{SM}}^2(t)}}\right), & \text{for } S_m > S_n, \\ Q\left(\frac{-S_{\bar{m}}h_{\bar{j}\hat{j}}(t)h_{\bar{j}j}(t+T_s) - S_m\sum_{i=1}^{N}h_{i\hat{j}}(t)h_{ij}(t) + \frac{(S_m+S_n)}{2}\sum_{i=1}^{N}h_{i\hat{j}}^2(t)}{\sqrt{\sum_{i=1}^{N}h_{i\hat{j}}^2(t)\sigma_{ni,\,\mathrm{SM}}^2(t)}}\right), & \text{for } S_m < S_n. \end{cases} \tag{41}$$

$$\Pr[S_m \to S_n|S_{\bar{m}}^{\bar{j}}, j] = \Pr\left[\sum_{i=1}^{N}|y_{i,\,\mathrm{SM}}(t) - S_m h_{ij}(t)|^2 > \sum_{i=1}^{N}|y_{i,\,\mathrm{SM}}(t) - S_n h_{ij}(t)|^2 \Big| S_{\bar{m}}^{\bar{j}}\right]$$
$$= \begin{cases} 1 - Q\left(\frac{-S_{\bar{m}}h_{\bar{j}\hat{j}}(t)h_{\bar{j}j}(t+T_s) + \frac{S_n-S_m}{2}\sum_{i=1}^{N}h_{ij}^2(t)}{\sqrt{\sum_{i=1}^{N}h_{ij}^2(t)\sigma_{ni,\,\mathrm{SM}}^2(t)}}\right), & \text{for } S_m > S_n, \\ Q\left(\frac{-S_{\bar{m}}h_{\bar{j}\hat{j}}(t)h_{\bar{j}j}(t+T_s) + \frac{S_n-S_m}{2}\sum_{i=1}^{N}h_{ij}^2(t)}{\sqrt{\sum_{i=1}^{N}h_{ij}^2(t)\sigma_{ni,\,\mathrm{SM}}^2(t)}}\right), & \text{for } S_m < S_n. \end{cases} \tag{42}$$

Finally, the average SER of the SM-MC systems can be approximately evaluated as

$$P_{e,\,\mathrm{SM}} = \frac{1}{M^2N^2}\sum_{j=1}^{N}\sum_{m=0}^{M-1}\sum_{\bar{j}=1}^{N}\sum_{\bar{m}=0}^{M-1}P_{e,\,\mathrm{SM}}(S_m^j|S_{\bar{m}}^{\bar{j}}). \tag{45}$$

## IV. Numerical Results

In this section, we present the analytical and simulation results for the SERs of the SSK-MC and SM-MC systems. Performance comparison among various modulation schemes and different detection schemes are also provided.

The definition of SNR in SISO-MC has been proposed in [37] when the OOK modulation scheme is considered. Here, we generalize the SNR definition to the $N \times N$ SM-MC and MIMO-MC with $M$-ary CSK modulation. Specifically, in SM-MC, the SNR can be defined similar to SISO-MC, as the ratio between the average received power of the desired link from a single transmitted impulse of molecules and the noise power, expressed as

$$\mathrm{SNR} = \frac{P_s}{P_n} = \frac{1}{MN}\sum_{j=1}^{N}\sum_{m=0}^{M-1}S_m h_{jj}(t_p)V_{\mathrm{RX}}$$
$$= \left(\frac{3}{2\pi e}\right)^{\frac{3}{2}}\frac{V_{\mathrm{RX}}}{Md^3}\sum_{m=0}^{M-1}S_m, \tag{46}$$

where $S_m > 0$ should be satisfied. As shown in (46), an SNR is dependent on the average number of molecules released by an impulse, the transceiver distance $d$ and the volume of receiver $V_{\mathrm{RX}}$. Similarly, the SNR of each link in the $N \times N$ MIMO-MC with $M$-ary CSK can be defined as

$$\mathrm{SNR} = \left(\frac{3}{2\pi e}\right)^{\frac{3}{2}}\frac{V_{\mathrm{RX}}}{NMd^3}\sum_{m=0}^{M-1}S_m. \tag{47}$$

Note that the SNR of (47) is $1/N$ of the that in (46), meaning that all the transmitters in MIMO-MC are activated to emit molecules during each symbol duration, under the constraint that the average number of molecules released per pulse is the same as that considered in (46).

When the transceiver distance $d$ is fixed, the same SNR implies the same molecular energy consumption. In this case, we can make relatively fair SER comparison between different modulation schemes for the MC with the same raw data rate and energy consumption. In order to achieve this, in our simulation for SM-MC with BCSK, we set $S_1 = 2S_0$. By contrast, for both SISO-MC and MIMO-MC with BCSK, we have $S_0 = 0$, meaning that the OOK modulation is applied. For SISO-MC with QCSK, we have $S_0 = 0$ and $S_3 = \frac{3}{2}S_2 = 3S_1$. The other system parameters are presented in Table II. Note that in this section, the SSK-MC with the $2\times2$ and $4\times4$ MIMO architectures are referred to as the BSSK-MC and QSSK-MC for brevity.

Fig. 4 shows the analytical and simulation results for the SER of the BSSK-MC and QSSK-MC, when the transceiver separation distance $r = 12.5$ $\mu$m and different symbol durations are considered. Clearly, the analytical SER agrees well with the corresponding simulated SER. In the low SNR region, the SER of QSSK-MC is much higher than that of the BSSK-MC, while in the high SNR region, the SER performance of QSSK-MC becomes better than that of the BSSK-MC, when $T_s = 0.1$ s and $T_s = 0.2$ s. By contrast, when $T_s = 0.8$ s, the SER of BSSK-MC is always lower than that of QSSK-MC in the whole SNR region considered. However, the gap between their SER performance decreases with the increase of SNR. As shown in Fig. 4, the SER performance of BSSK-MC and QSSK-MC is highly dependent on the symbol duration $T_s$ . When $T_s$ increases, the SER reduces due to the fact that the

TABLE II
System Parameters

| Parameter | Variable | Value | Unit |
|---|---|---|---|
| Diffusion Coefficient | $D$ | $2.2 \times 10^{-9}$ | $m^2/s$ |
| Link Distance | $d$ | $[15, 20, 25]$ | $\mu$m |
| Receiver Radius | $\rho$ | $0.1$ | $\mu$m |
| Order of Concentration Symbol | $M$ | $[2, 4]$ | |
| Order of Space Symbol | $N$ | $[2, 4]$ | |
| Symbol Sequence Length | | $5 \times 10^6$ | |
| Replication Times | | 20 | |

This article has been accepted for publication in a future issue of this journal, but has not been fully edited. Content may change prior to final publication. Citation information: DOI 10.1109/TNB.2019.2905254, IEEE Transactions on NanoBioscience



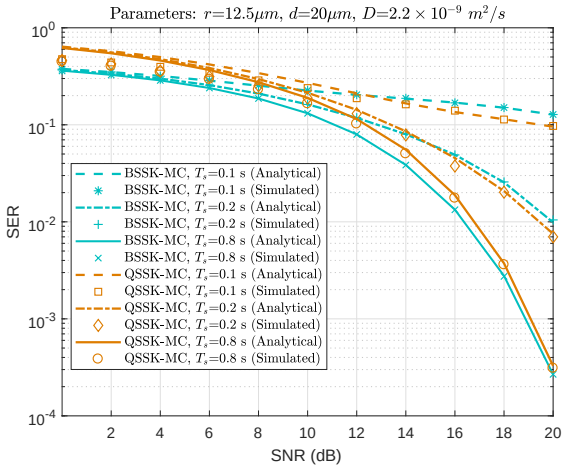


Fig. 4. SER comparison between BSSK-MC and QSSK-MC with non-coherent detection, when $T_s = 0.1$ s, $0.2$ s, $0.8$ s are assumed.

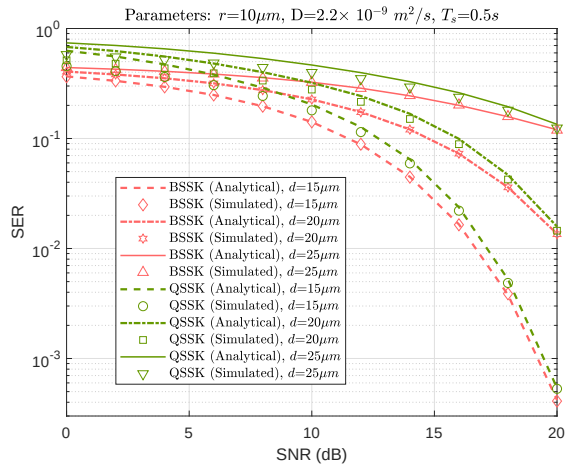


Fig. 6. SER comparison between BSSK-MC and QSSK-MC with non-coherent detection, when $d = 15$ $\mu$m, $20$ $\mu$m, $25$ $\mu$m are considered.

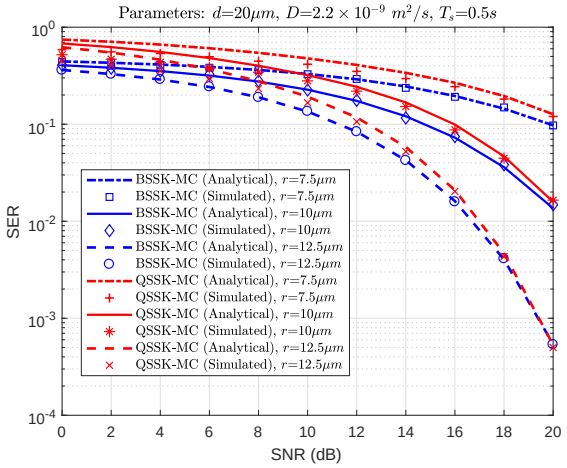


Fig. 5. SER comparison between BSSK-MC and QSSK-MC with non-coherent detection, when $r = 7.5$ $\mu$m, $10$ $\mu$m, $12.5$ $\mu$m are considered.

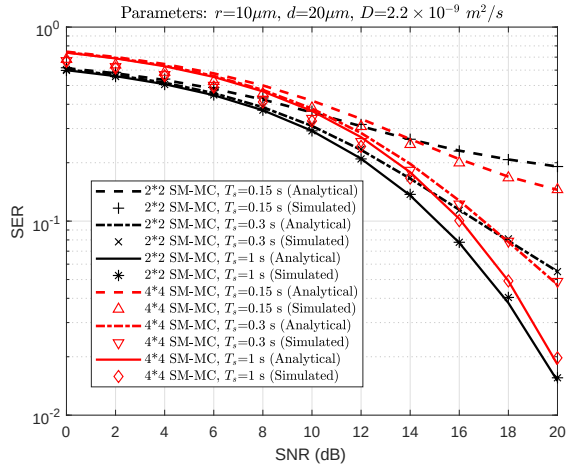


Fig. 7. SER comparison between the $2 \times 2$ SM-MC and $4 \times 4$ SM-MC with the MRC-assisted detection, when $T_s = 0.15$ s, $0.3$ s, $1$ s and BCSK modulation are assumed.

ISI reduces, with $T_s$ increasing.

Fig. 5 manifests the analytical and simulation SER of BSSK-MC and QSSK-MC, when different transceiver separation distances are considered. Again, the simulation and analytical results match well, which hence validate our theoretical analysis. As shown in the figure, for a given transceiver separation distance, there is a gap between the SER performance of BSSK-MC and that of QSSK-MC in the low SNR region, with BSSK-MC always outperforming the QSSK-MC. However, as the SNR increases, the SER curves of BSSK-MC and QSSK-MC converge and become nearly the same at high SNR. Therefore, when sufficient source of information molecules, i.e., high SNR, is available, higher throughput can be attained by utilizing higher order modulation schemes in the SSK-MC, while achieving the required error performance.

Various link distances are considered in Fig. 6, which shows a similar performance trend as Figs. 4 and 5. Again, good match between the analytical and simulated results is observed in Fig. 6. When the transceiver separation distance and symbol duration are fixed, a larger link distance deteriorates further the SER performance of both the BSSK-MC and QSSK-MC, indicating that the link distance plays a significant role in affecting the SER performance of MIMO-MC systems.

Fig. 7 depicts the theoretical SER upper bound and the simulated SER of the SM-MC with BCSK modulation, when both the $2 \times 2$ and the $4 \times 4$ MIMO architectures are respectively considered. In this figure, the transceiver separation distance is fixed to $r = 10$ $\mu$m, whilst the symbol durations $T_s$ is set to $0.15$ s, $0.3$ s or $1$ s. The results show that the upper bound is tight, which becomes tighter as the SNR increases. As shown in Fig. 7, in the low SNR regime, the SER of the $4 \times 4$ SM-MC with BCSK modulation is much higher than that of the $2 \times 2$ SM-MC with BCSK modulation. By contrast, in the high SNR regime, the SER of the $4 \times 4$ SM-MC is better than that of the $2 \times 2$ SM-MC, when $T_s = 0.15$ s or $T_s = 0.3$ s. Furthermore, when $T_s = 1$ s, the SER of the $2 \times 2$ SM-MC is always lower than that of the $4 \times 4$ SM-MC in the SNR region considered. The explanation for these results are similar to that for the results shown in Fig. 4.

This article has been accepted for publication in a future issue of this journal, but has not been fully edited. Content may change prior to final publication. Citation information: DOI 10.1109/TNB.2019.2905254, IEEE Transactions on NanoBioscience



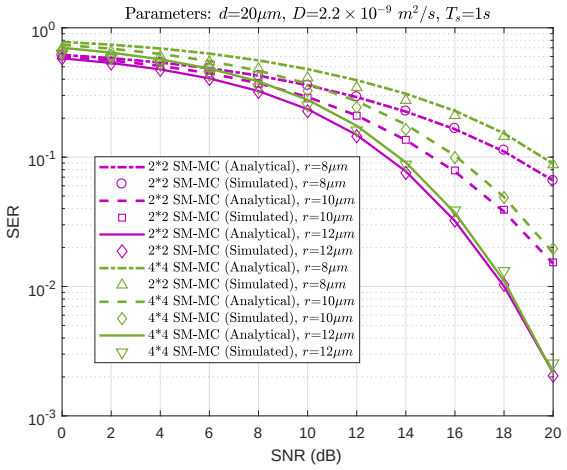


Fig. 8. SER comparison between the $2 \times 2$ SM-MC and $4 \times 4$ SM-MC with the MRC-assisted detection, when $r = 8\ \mu\text{m}, 10\ \mu\text{m}, 12\ \mu\text{m}$ and BCSK modulation are considered.

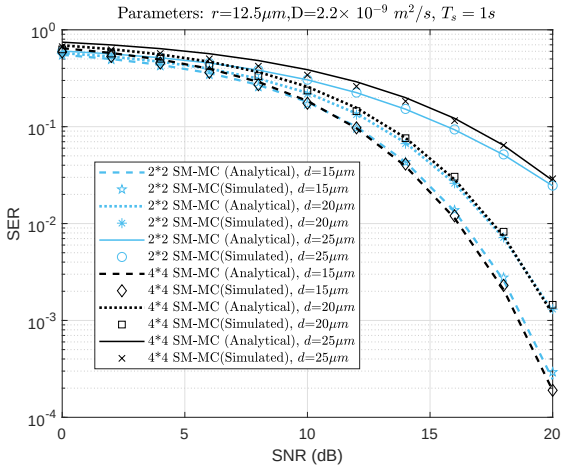


Fig. 9. SER comparison between the $2 \times 2$ SM-MC and $4 \times 4$ SM-MC with the MRC-assisted detection, when $d = 15\ \mu\text{m}, 20\ \mu\text{m}, 25\ \mu\text{m}$ are considered.

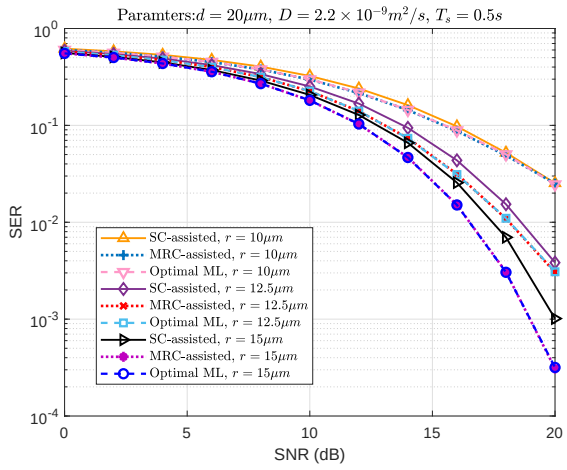


Fig. 10. SER performance comparison of the $2 \times 2$ SM-MC employing ML, MRC-assisted or SC-assisted detection, when $r = 10\ \mu\text{m}, 12.5\ \mu\text{m}$ or $15\ \mu\text{m}$ and BCSK modulation are considered.

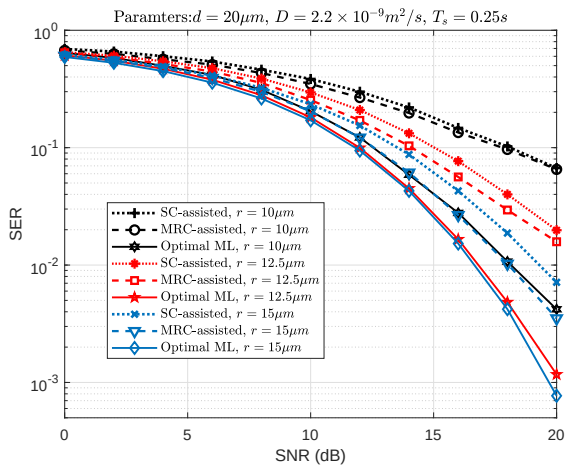


Fig. 11. SER performance comparison of the $4 \times 4$ SM-MC employing ML, MRC-assisted or SC-assisted detection, when $r = 10\ \mu\text{m}, 12.5\ \mu\text{m}$ or $15\ \mu\text{m}$ and BCSK modulation are considered.

Fig. 8 also demonstrates the theoretical SER upper bound and the simulation SER results of the SM-MC employing with BCSK modulation, where the symbol duration is set to $T_s = 1$ s, while various transceiver separation distances are considered. Similar to Fig. 7, the SER upper bounds agree well with their corresponding results obtained from simulations. There is also an SER gap between the $2 \times 2$ SM-MC and its $4 \times 4$ counterpart. However, when the transceiver separation distance increases, the SER difference between the $2 \times 2$ and $4 \times 4$ SM-MC reduces. Here we should note that when the link distance $d$ and the symbol duration $T_s$ are fixed, the SER performance of SM-MC is mainly determined by the transceiver separation distance $r$.

Fig. 9 shows the SER performance of the $2 \times 2$ and $4 \times 4$ SM-MC with different link distances, where similar observations as from Fig. 6 can be derived. The SER performance of the $2 \times 2$ and $4 \times 4$ SM-MC employing various detection schemes are compared in Figs. 10 and 11, respectively. In these schemes, the optimal ML detection based on (28), and the two suboptimal detection schemes, i.e., SC-assisted and MRC-assisted detectors based on (29), (33) and (34) are considered. Specifically, in Fig. 10, the symbol duration $T_s$ is set to 0.5 s, and $N = 2$ and $M = 2$, forming a $2 \times 2$ SM-MC with BCSK modulation. Therefore, the complexity of the optimal ML detector is similar to that of the suboptimal detectors. From Fig. 10, we observe that the SC-assisted detector achieves the worst SER performance among the three detection schemes, which become more declared, as $r$ increases. Fig. 10 shows that the SER performance of the MRC-assisted detector is nearly the same as that of the optimal ML detector regardless of the separation distances. This agrees with our previous argument in Section III. Both the optimal ML and the MRC-assisted detectors exploit all the received signals to decode the space and concentration symbols, although the MRC-assisted detector carries out separable detection, while the ML detector executes joint detection.

By contrast, for the $4 \times 4$ SM-MC with BCSK modulation, the optimal ML detector always outperforms the other two

This article has been accepted for publication in a future issue of this journal, but has not been fully edited. Content may change prior to final publication. Citation information: DOI 10.1109/TNB.2019.2905254, IEEE Transactions on NanoBioscience



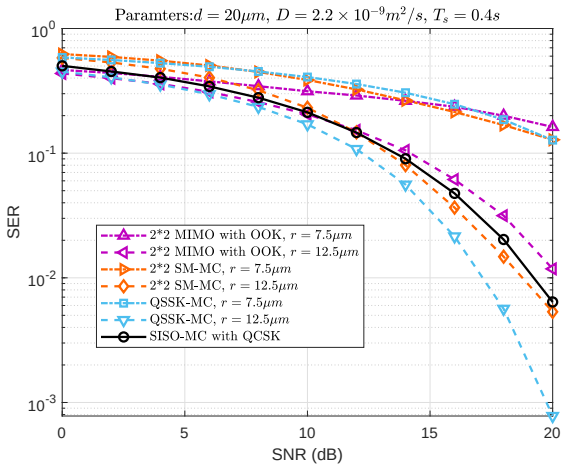


Fig. 12. Comparison of the SER of the QSSK-MC with non-coherent detection and the SM-MC with MRC-assisted detection with that of the MIMO-MC with OOK modulation and that of the SISO-MC with QCSK modulation, when $r = 7.5$ $\mu$m or $12.5$ $\mu$m.

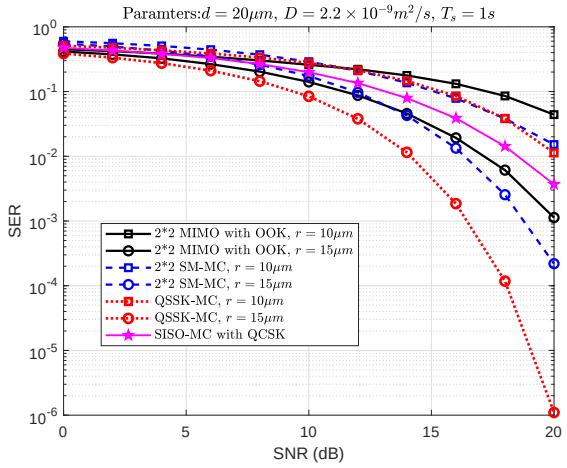


Fig. 13. Comparison of the SER of the QSSK-MC with non-coherent detection and the SM-MC under MRC-assisted detector with that of the MIMO-MC with OOK modulation and that of the SISO-MC with QCSK modulation, when $r = 10$ $\mu$m or $15$ $\mu$m.

suboptimal detections as shown in Fig. 11. where the symbol duration $T_s$ is set as $0.25$ s. Note that since for Fig. 11 $N = 4$ and $M = 2$, the search complexity of the suboptimal detectors is lower than that of the optimal ML detector. Due to the suboptimal separate detection, as shown in Fig. 11, the SER performance of the MRC-assisted detector is worse than that of the optimal ML detector, and the SC-assisted detector exhibits the worst SER performance. However, as $r$ increases, the SER difference between the ML and MRC-assisted detectors becomes smaller, while that between the MRC-and SC-assisted detectors becomes larger. In more detail, as shown in Fig. 11, the MRC-assisted detector only slightly outperforms the SC-assisted SM-MC when $r = 10$ $\mu$m, whereas in this case, the optimal ML detector is capable of providing about $6$ dB gain above the two suboptimal detectors. When $r = 12.5$ $\mu$m, the performance gap between the ML and the MRC-assisted detectors is decreased to $4$ dB, while the MRC-assisted detector is about $1$ dB better than the SC-assisted detector. Finally, when $r = 15$ $\mu$m, the performance gain of the MRC-assisted detector over the SC-assisted detector becomes $1.5$ dB in the high SNR region, whilst the performance gap between the optimal ML detector and MRC-assisted detector is further reduced to about $2$ dB.

To verify the effectiveness of our proposed SSK-MC and SM-MC, we compare the SER performance among the SISO-MC with QCSK, $2 \times 2$ MIMO-MC with OOK, QSSK-MC and the $2 \times 2$ SM-MC with BCSK in Figs. 12 and 13, when the symbol durations $T_s$ is set as $0.4$ s (Fig. 12) and $1$ s (Fig. 13), respectively. As seen above, all considered schemes have the same raw data rate of 2 bits per symbol. In these schemes, the QSSK-MC assumes the non-coherent detection scheme shown in (29).

The $2 \times 2$ SM-MC uses the MRC-assisted suboptimal detection based on (29) and (34), while the detection schemes for the SISO-MC and the $2 \times 2$ MIMO-MC are given in [9], [18]. As shown in Figs. 10 and 11, when the separation distance between the transmitters (also the receivers) is

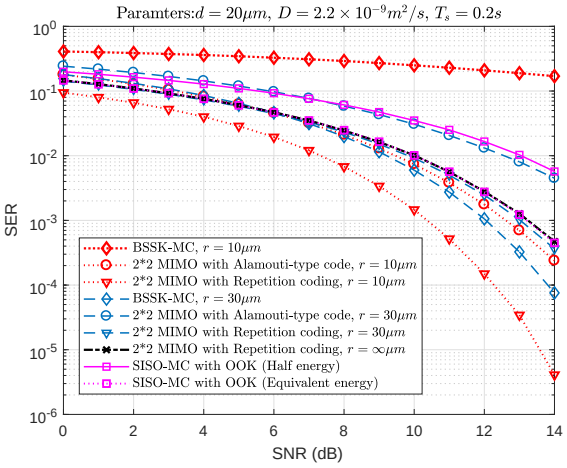


Fig. 14. Comparison of the SER of the BSSK-MC with non-coherent detection with that of the MIMO-MC using repetition coding or using Alamouti-type coding as well as that of the SISO-MC with OOK modulation, when $r = 10$ $\mu$m or $30$ $\mu$m.

relatively large, such as, $r = 12.5$ $\mu$m, $r = 15$ $\mu$m, the QSSK-MC outperforms all the other schemes and achieves the best SER performance. Both the SSK-MC and SM-MC can benefit from the employment of space modulation, making them significantly surpass the $2 \times 2$ MIMO-MC in the high SNR regime. As shown in Figs. 12 and 13, the SISO-MC with QCSK attains the worst SER performance among the schemes considered. However, the situation is completely different when the separation distance is reduced to $r = 7.5$ $\mu$m or to $r = 10$ $\mu$m. In these cases, the SISO-MC with QCSK achieves the lowest SER and outperforms all the other MIMO-MC schemes. The $2 \times 2$ MIMO-MC with OOK has a similar SER performance as the QSSK-MC and the $2 \times 2$ SM-MC, when the SNR is low. While increasing the SNR to a sufficient value, the SER performance of the conventional $2 \times 2$ MIMO-MC becomes poorer than the SM-MC and SSK-MC schemes.

The results in both Figs. 12 and 13 show a similar trend,

implying that the separation distance $r$ imposes an important impact on the achievable SER performance of the MIMO-MC schemes when comparing them with SISO-MC. As shown in these figures, when $r$ is appropriately selected, the MIMO-MC schemes are capable of outperforming the SISO-MC with QCSK, resulting in insignificant ILI in the MIMO-MC schemes, which is beneficial to transmitting information by exploiting the space domain degrees of freedom. By contrast, if $r$ is small, yielding significant ILI, the advantage provided by the space domain vanishes.

Finally, in Fig. 14, we compare the SER performance when the MIMO-MC assisted by spatial diversity is considered [24]. Specifically, we compare the SER performance of the BSSK-MC, with that of the MIMO-MC with the spatial diversity based on repetition coding and Alamouti-type coding. Furthermore, the SER of the SISO-MC with OOK is depicted as a benchmark in Fig. 14. We assume that the ML detection is implemented for the MIMO-MC with repetition coding and Alamouti-type coding, while the BSSK-MC adopts the non-coherent detection scheme of (29) and the SISO-MC with OOK uses the threshold-assisted detection [33]. Additionally, all these schemes have the same raw data rate of 1 bit per symbol. As shown in Fig. 14, explicitly, the error performance of these schemes is highly dependent on the transceiver separation distance $r$. When $r = 10\ \mu\mathrm{m}$, the MIMO-MC with repetition coding attains the best SER performance among these schemes with the same transceiver separation distance, as the result that the ILI in the repetition coding plays a constructive role to enhance the signal strength at the receiver. The SER performance of the MIMO-MC with Alamouti-type coding falls between that of the repetition coding assisted scheme and that of the BSSK-MC, while the SSK-MC shows the worst SER performance, due to strong ILI, which results in that the receiver is unable to distinguish the activated transmitter index. By contrast, when $r = 30\ \mu\mathrm{m}$, the effect of ILI is significantly decreased because of the larger transceiver separation. Correspondingly, the SER performance of BSSK-MC is significantly improved, becoming better than that of the other schemes. The repetition coding scheme is inferior to the BSSK-MC in terms of SER, but still provides a desirable SER performance, but the Alamouti-type coding scheme has the poorest SER performance. Furthermore, the SER performance of the repetition coding scheme with $r = 30\ \mu\mathrm{m}$ is only slightly better than its counterpart with $r = \infty\ \mu\mathrm{m}$, yielding zero ILI. Hence, the effect of ILI in the case of $r = 30\ \mu\mathrm{m}$ is extremely small. As shown in Fig. 14, the SER performance of the repetition coding scheme without ILI ($r = \infty\ \mu\mathrm{m}$) coincides with that of the SISO-MC with OOK, when the same average number of molecules per symbol is emitted. Moreover, when the average number of molecules per symbol is halved, the SER performance of SISO-MC has exact 3 dB loss.

From the results of Fig. 14, we are implied that the ILI effect should be considered for selecting a MIMO-MC scheme in order to achieve the highest reliability. When the ILI is relatively strong, the repetition coding scheme is preferred to exploit the ILI. Otherwise, if the ILI is sufficiently weak, the SSK-MC is desirable for reliable data transmission.

Additionally, based on the performance shown in this paper, in order to improve the SER performance of the SSK-MC and that of SM-MC, the following approaches may be applied. Firstly, the symbol duration $T_s$ may be increased to reduce ISI, which improves the SER of the SSK-MC and SM-MC systems, but at the cost of transmission rate. Secondly, the separation distance between adjacent transmitters and that between adjacent receivers can be increased for mitigating the ILI. This is an effective method to improve the SER performance provided that there are spaces for deployment of transmitters and receivers. Furthermore, we may increase the number of molecules per pulse to increase SNR, which therefore enhances the reliability of information transmission, but at the cost of energy consumption.

## V. Conclusions and Future Work

In this paper, we have proposed an SM-MC scheme and its special case of SSK-MC by introducing new degrees of freedom from the spatial domain to transmit more information in MC. Our studies have shown that when the separation distance between transmit/receive nanomachines is appropriate, additional information conveyed in the space domain is achievable, and our proposed SSK-MC and SM-MC are capable of outperforming the conventional SISO-MC and MIMO-MC schemes. The reason behind is that our proposed SM-MC can effectively mitigate the ILI, which usually severely affects the performance of the conventional MIMO-MC. Moreover, as only one nanomachine transmitter is activated during each symbol period, SM-MC has twofold of benefit for small-scale MC communication systems, which are the high energy efficiency and low complexity.

In this paper, we have considered the memoryless receivers, where short ILI and ISI are assumed. Nevertheless, the ISI and ILI tend to be long in practical situations, which may severely affect the system performance of MC. In our future work, we will extend our study and consider the effective methods to overcome long ILI in MIMO-MC. For this purpose, besides sharing the knowledge among the nanomachine receivers with finite memory for ILI mitigation, other ILI reducing techniques may be designed based on the properties of MIMO-MC.

## Appendix A

Let us denote $\Pr_{\mathrm{SSK}}[i|S_{\bar{m}}^{\bar{j}}]$ as the probability that the $i$-th receiver senses the maximum molecular concentration, which can be expressed as

$$\Pr_{\mathrm{SSK}}[i|S_{\bar{m}}^{\bar{j}}] = \Pr\Big[\big(y_{i,\,\mathrm{SM}}(t) > y_{1,\,\mathrm{SM}}(t)\big) \cap \cdots \cap \big(y_{i,\,\mathrm{SM}}(t) > y_{N,\,\mathrm{SM}}(t)\big)\Big], \tag{48}$$

when given that the previously sent molecular symbol is $S_{\bar{m}}^{\bar{j}}$. In order to derive the error detection probability of the space symbol, let us first derive the correct detection probability of the space symbol, when $S_m$ molecules are released from the $j$-th transmitter. Based on (48), this probability can be expressed as

$$\begin{aligned} P_{c,\,\mathrm{SSK}}(S_m^j|S_{\bar{m}}^{\bar{j}}) &= \Pr_{\mathrm{SSK}}[j|S_{\bar{m}}^{\bar{j}}] \\ &= \Pr\Big[\big(y_{j,\,\mathrm{SM}}(t) > y_{1,\,\mathrm{SM}}(t)\big) \cap \cdots \cap \big(y_{j,\,\mathrm{SM}}(t) > y_{N,\,\mathrm{SM}}(t)\big)\Big], \end{aligned} \tag{49}$$

which is the probability that the $j$-th receiver senses the maximum concentration. When the receiving processes of different nanomachines are assumed to be independent, (49) can be expressed as

$$P_{c,\,\mathrm{SSK}}(S_m^j|S_{\bar{m}}^{\bar{j}}) = \prod_{i\neq j} \Pr[y_{j,\,\mathrm{SM}}(t) - y_{i,\,\mathrm{SM}}(t) > 0|S_{\bar{m}}^{\bar{j}}]. \quad (50)$$

Furthermore, when given $S_{\bar{m}}^{\bar{j}}$, the term $y_{j,\,\mathrm{SM}}(t) - y_{i,\,\mathrm{SM}}(t)$ can be written as

$$\begin{aligned} y_{ji|S_{\bar{m}}^{\bar{j}}} =& S_m\big(h_{jj}(t) - h_{ij}(t)\big) + I_{j,\,\mathrm{SM}}(t) - I_{i,\,\mathrm{SM}}(t) \\ &+ n_{j,\,\mathrm{SM}}(t) - n_{i,\,\mathrm{SM}}(t). \end{aligned} \quad (51)$$

According to (25), $y_{ji|S_{\bar{m}}^{\bar{j}}}$ follows the Normal distribution of

$$y_{ji|S_{\bar{m}}^{\bar{j}}} \sim \mathcal{N}\left(\mu_{ji|S_{\bar{m}}^{\bar{j}}}, \sigma^2_{ji|S_{\bar{m}}^{\bar{j}}}\right). \quad (52)$$

When given $i \neq j$, and according to [48], $\mu_{ji|S_{\bar{m}}^{\bar{j}}}$ and $\sigma^2_{ji|S_{\bar{m}}^{\bar{j}}}$ are given by

$$\mu_{ji|S_{\bar{m}}^{\bar{j}}} = \begin{cases} S_m\big(h_{jj}(t) - h_{ij}(t)\big) - S_{\bar{m}} h_{ii}(t+T_s), & \text{for } i=\bar{j} \text{ and } j\neq\bar{j}, \\ S_m\big(h_{jj}(t) - h_{ij}(t)\big) + S_{\bar{m}} h_{jj}(t+T_s), & \text{for } i\neq\bar{j} \text{ and } j=\bar{j}, \\ S_m\big(h_{jj}(t) - h_{ij}(t)\big), & \text{for } i\neq\bar{j} \text{ and } j\neq\bar{j}, \end{cases} \quad (53)$$

$$\sigma^2_{ji|S_{\bar{m}}^{\bar{j}}} = \begin{cases} \frac{S_m\left(h_{jj}(t) + h_{ij}(t)\right) + S_{\bar{m}} h_{ii}(t+T_s)}{V_{\mathrm{RX}}}, & \text{for } i=\bar{j} \text{ and } j\neq\bar{j}, \\ \frac{S_m\left(h_{jj}(t) + h_{ij}(t)\right) + S_{\bar{m}} h_{jj}(t+T_s)}{V_{\mathrm{RX}}}, & \text{for } i\neq\bar{j} \text{ and } j=\bar{j}, \\ \frac{S_m\left(h_{jj}(t) + h_{ij}(t)\right)}{V_{\mathrm{RX}}}, & \text{for } i\neq\bar{j} \text{ and } j\neq\bar{j}, \end{cases} \quad (54)$$

respectively. Therefore, we have

$$\begin{aligned} \Pr[y_{ji|S_{\bar{m}}^{\bar{j}}} > 0] &= \int_0^{+\infty} \frac{1}{\sqrt{2\pi}\sigma_{ji|S_{\bar{m}}^{\bar{j}}}} \exp\left(-\frac{(y_{ji|S_{\bar{m}}^{\bar{j}}} - \mu_{ji|S_{\bar{m}}^{\bar{j}}})^2}{2\sigma^2_{ji|S_{\bar{m}}^{\bar{j}}}}\right) dy_{ji|S_{\bar{m}}^{\bar{j}}} \\ &= Q\left(-\frac{\mu_{ji|S_{\bar{m}}^{\bar{j}}}}{\sigma_{ji|S_{\bar{m}}^{\bar{j}}}}\right). \end{aligned} \quad (55)$$

Finally, when substituting (55) into (50), the probability of correct detection of the space symbol $j$ can be formulated as

$$P_{c,\,\mathrm{SSK}}(S_m^j|S_{\bar{m}}^{\bar{j}}) = \prod_{i\neq j} Q\left(-\frac{\mu_{ji|S_{\bar{m}}^{\bar{j}}}}{\sigma_{ji|S_{\bar{m}}^{\bar{j}}}}\right). \quad (56)$$

## REFERENCES


[1] H. H. Shorey, *Animal Communication by Pheromones*. Academic Press, 2013.

[2] I. Akyildiz, F. Fekri, R. Sivakumar, C. Forest, and B. Hammer, "MONACO: Fundamentals of molecular nano-communication networks," *IEEE Wireless Commun.*, vol. 19, no. 5, pp. 12–18, Oct. 2012.

[3] J. T. Hancock, *Cell Signalling*. Oxford University Press, 2017.

[4] T. Nakano *et al.*, "Molecular communication for nanomachines using intercellular calcium signaling," in *Proc. 5th IEEE Conf. on Nanotechnology*, Nagoya, Japan, July 2005, pp. 478–481.

[5] N. Farsad *et al.*, "A comprehensive survey of recent advancements in molecular communication," *IEEE Commun. Survey & Tut.*, vol. 18, no. 3, pp. 1887–1919, third quarter 2016.

[6] J. Wang, *Nanomachines: Fundamentals and Applications*. Wiley, 2013.

[7] T. Nakano, "Molecular communication: A 10 year retrospective," *IEEE Trans. Mol. Biol. Multi-Scale Commun.*, vol. 3, no. 2, pp. 71–78, June 2017.

[8] J. Suzuki, T. Nakano, and M. J. Moore, *Modeling, Methodologies and Tools for Molecular and Nano-scale Communications: Modeling, Methodologies and Tools*. Springer International Publishing, 2017.

[9] M. S. Kuran, H. B. Yilmaz, T. Tugcu, and I. F. Akyildiz, "Modulation techniques for communication via diffusion in nanonetworks," in *Proc. IEEE Int. Conf. on Commun. (ICC)*, Kyoto, Japan, June 2011, pp. 1–5.

[10] N. R. Kim and C.-B. Chae, "Novel modulation techniques using isomers as messenger molecules for nano communication networks via diffusion," *IEEE J. Sel. Areas Commun.*, vol. 31, no. 12, pp. 847–856, Dec. 2013.

[11] I. Llatser, A. Cabellos-Aparicio, M. Pierobon, and E. Alarcon, "Detection techniques for diffusion-based molecular communication," *IEEE J. Sel. Areas Commun.*, vol. 31, no. 12, pp. 726–734, Dec. 2013.

[12] H. Arjmandi, A. Gohari, M. N. Kenari, and F. Bateni, "Diffusion-based nanonetworking: A new modulation technique and performance analysis," *IEEE Commun. Lett.*, vol. 17, no. 4, pp. 645–648, Apr. 2013.

[13] M. H. Kabir, S. M. R. Islam, and K. S. Kwak, "D-MoSK modulation in molecular communications," *IEEE Trans. Nanobiosci.*, vol. 14, no. 6, pp. 680–683, Sept. 2015.

[14] R. Mosayebi, A. Gohari, M. Mirmohseni, and M. Nasiri-Kenari, "Type-based sign modulation and its application for ISI mitigation in molecular communication," *IEEE Trans. on Commun.*, vol. 66, no. 1, pp. 180–193, Jan. 2018.

[15] H. B. Yilmaz, G. Suk, and C. Chae, "Chemical propagation pattern for molecular communications," *IEEE Wireless Commun. Lett.*, vol. 6, no. 2, pp. 226–229, Apr. 2017.

[16] Y. Huang, M. Wen, C. Lee, C. Chae, and F. Ji, "A two-way molecular communication assisted by an impulsive force," *IEEE Trans. Ind. Informat.*, pp. 1–1, 2019.

[17] P. C. Yeh *et al.*, "A new frontier of wireless communication theory: Diffusion-based molecular communications," *IEEE Wireless Commun.*, vol. 19, no. 5, pp. 28–35, Oct. 2012.

[18] L. S. Meng, P. C. Yeh, K. C. Chen, and I. F. Akyildiz, "MIMO communications based on molecular diffusion," in *Proc. IEEE Global Commun. Conf. (GLOBECOM)*, Anaheim, CA, USA, Dec. 2012, pp. 5380–5385.

[19] T. Nakano, A. W. Eckford, and T. Haraguchi, *Molecular Communication*. Cambridge University Press, 2013.

[20] N. Farsad, W. Guo, and A. W. Eckford, "Tabletop molecular communication: Text messages through chemical signals," *PLOS ONE*, vol. 8, pp. 1–13, Dec. 2013.

[21] B. H. Koo *et al.*, "Molecular MIMO: From theory to prototype," *IEEE J. Sel. Areas Commun.*, vol. 34, no. 3, pp. 600–614, Mar. 2016.

[22] C. Lee, H. B. Yilmaz, C.-B. Chae, N. Farsad, and A. Goldsmith, "Machine learning based channel modeling for molecular MIMO communications," in *Proc. IEEE 18th International Workshop on Signal Processing Advances in Wireless Communi. (SPAWC)*, Sapporo, Japan, July 2017, pp. 1–5.

[23] S. M. Rouzegar and U. Spagnolini, "Channel estimation for diffusive MIMO molecular communications," in *Proc. European Conf. on Networks and Communi. (EuCNC)*, Oulu, Finland, June 2017, pp. 1–5.

[24] M. Damrath, H. B. Yilmaz, C. Chae, and P. A. Hoeher, "Array gain analysis in molecular MIMO communications," *IEEE Access*, vol. 6, pp. 61 091–61 102, 2018.

[25] Z. Luo *et al.*, "One symbol blind synchronization in SIMO molecular communication systems," *IEEE Wireless Commun. Lett.*, vol. 7, no. 4, pp. 530–533, Aug. 2018.

[26] M. A. Mangoud, M. Lestas, and T. Saeed, "Molecular motors MIMO communications for nanonetworks applications," in *Proc. IEEE Wireless Commun. and Netw. Conf. (WCNC)*, Barcelona, Spain, Apr. 2018, pp. 1–5.

[27] E. G. Larsson, O. Edfors, F. Tufvesson, and T. L. Marzetta, "Massive MIMO for next generation wireless systems," *IEEE Commun. Mag.*, vol. 52, no. 2, pp. 186–195, Feb. 2014.

[28] M. D. Renzo *et al.*, "Spatial modulation for generalized MIMO: Challenges, opportunities, and implementation," *Proc. IEEE*, vol. 102, no. 1, pp. 56–103, Jan. 2014.

[29] R. Y. Mesleh *et al.*, "Spatial modulation," *IEEE Trans. Veh. Technol.*, vol. 57, no. 4, pp. 2228–2241, July 2008.

[30] J. Jeganathan, A. Ghrayeb, L. Szczecinski, and A. Ceron, "Space shift keying modulation for MIMO channels," *IEEE Trans. Wireless Commun.*, vol. 8, no. 7, pp. 3692–3703, July 2009.

[31] E. Basar *et al.*, "Index modulation techniques for next-generation wireless networks," *IEEE Access*, vol. 5, pp. 16 693–16 746, 2017.

[32] M. D. Renzo and H. Haas, "Bit error probability of SM-MIMO over generalized fading channels," *IEEE Trans. Veh. Technol.*, vol. 61, no. 3, pp. 1124–1144, Mar. 2012.
[33] A. Aijaz and A. Aghvami, "Error performance of diffusion-based molecular communication using pulse-based modulation," *IEEE Trans. Nanobiosci.*, vol. 14, no. 1, pp. 146–151, Jan. 2015.
[34] B. Tepekule *et al.*, "ISI mitigation techniques in molecular communication," *IEEE Trans. Mol. Biol. Multi-Scale Commun.*, vol. 1, no. 2, pp. 202–216, June 2015.
[35] S. K. Tiwari and P. K. Upadhyay, "Maximum likelihood estimation of SNR for diffusion-based molecular communication," *IEEE Wireless Commun. Lett.*, vol. 5, no. 3, pp. 320–323, June 2016.
[36] Y. Zamiri-Jafarian, S. Gazor, and H. Zamiri-Jafarian, "Molecular code division multiple access in nano communication systems," in *Proc. IEEE Wireless Communi. and Netw. Conf.*, Doha, Qatar, Apr. 2016, pp. 1–6.
[37] L. Shi and L. Yang, "Error performance analysis of diffusive molecular communication systems with On-Off Keying modulation," *IEEE Trans. Mol. Biol. Multi-Scale Commun.*, vol. 3, no. 4, pp. 224–238, Dec. 2017.
[38] M. U. Mahfuz, D. Makrakis, and H. T. Mouftah, "A comprehensive study of sampling-based optimum signal detection in concentration-encoded molecular communication," *IEEE Trans. Nanobiosci.*, vol. 13, no. 3, pp. 208–222, Sept. 2014.
[39] G. Chang, L. Lin, and H. Yan, "Adaptive detection and ISI mitigation for mobile molecular communication," *IEEE Trans. Nanobiosci.*, vol. 17, no. 1, pp. 21–35, Mar. 2018.
[40] L. S. Meng, P. C. Yeh, K. C. Chen, and I. F. Akyildiz, "On receiver design for diffusion-based molecular communication," *IEEE Trans. Signal Process.*, vol. 62, no. 22, pp. 6032–6044, Nov. 2014.
[41] M. S. Kuran, H. B. Yilmaz, T. Tugcu, and B. . Edis, "Energy model for communication via diffusion in nanonetworks," *Nano Communication Networks*, vol. 1, pp. 86–95, 06 2010.
[42] N. R. Kim, A. W. Eckford, and C.-B. Chae, "Symbol interval optimization for molecular communication with drift," *IEEE Trans. Nanobiosci.*, vol. 13, no. 3, pp. 223–229, Sept. 2014.
[43] H. Kwon and T. Birdsall, "Channel capacity in bits per joule," *IEEE J. Ocean. Eng.*, vol. 11, no. 1, pp. 97–99, Jan. 1986.
[44] J. Jeganathan, A. Ghrayeb, and L. Szczecinski, "Spatial modulation: optimal detection and performance analysis," *IEEE Commun. Lett.*, vol. 12, no. 8, pp. 545–547, Aug. 2008.
[45] C. Xu, S. Sugiura, S. X. Ng, and L. Hanzo, "Spatial modulation and space-time shift keying: Optimal performance at a reduced detection complexity," *IEEE Trans. Commun.*, vol. 61, no. 1, pp. 206–216, Jan. 2013.
[46] R. Zhang, L. L. Yang, and L. Hanzo, "Generalised pre-coding aided spatial modulation," *IEEE Trans. Wireless Commun.*, vol. 12, no. 11, pp. 5434–5443, Nov. 2013.
[47] M. Maleki, H. R. Bahrami, and A. Alizadeh, "On MRC-based detection of spatial modulation," *IEEE Trans. Wireless Commun.*, vol. 15, no. 4, pp. 3019–3029, Apr. 2016.
[48] J. Patel and C. Read, *Handbook of the Normal Distribution, Second Edition*. Taylor & Francis, 1996.

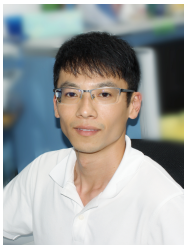

**Yu Huang** was born in Zhejiang, China. He received the B.S. degree in communication engineering from Harbin University of Science and Technology, Harbin, China, in 2016. He is currently a Ph. D. candidate in information and communication engineering at South China University of Technology, Guangzhou, China. From July to August in 2018, he was a visiting student for molecular communication in Yonsei University, Seoul, South Korea. His main research interests include molecular communications, physical layer security, and wireless communication in challenged environments.

**Miaowen Wen** (M'14 - SM'18) received his Ph.D. degree in Signal and Information Processing from Peking University, China, in 2014. From 2012 to 2013, he was a Visiting Student Research Collaborator with Princeton University, USA. He is currently an Associate Professor with the South China University of Technology, China, and a Post-doctoral Fellow with The University of Hong Kong, China. He has published over 100 research papers, including over 60 journal papers. His research interests include index modulation, non-orthogonal multiple access, physical layer security, and molecular communications.

**Lie-Liang Yang** (M'98 - SM'02 - F'16) is the professor of wireless communications in the University of Southampton. He has research interest in wireless communications, wireless networks and signal processing for wireless communications, as well as molecular communications and nano-networks. He has published over 370 research papers, authored/co-authored three books and a number of book chapters. He is a fellow of both the IEEE and the IET. He served as an associate editor to the IEEE Trans. on Vehicular Technology and Journal of Communications and Networks (JCN), and is currently an associate editor of IEEE Access and an subject editor of IET Electronics Letters.

**Chan-Byoung Chae** (S'06 - M'09 - SM'12) is the Underwood Distinguished Professor in the School of Integrated Technology, Yonsei University. He received his Ph.D. degree in electrical and computer engineering from The University of Texas at Austin in 2008, where he was a member of the Wireless Networking and Communications Group (WNCG).

He is now the Editor-in-Chief of the *IEEE Trans. Molecular, Biological, and Multi-scale Communications*. He has served/serves as an Editor for the *IEEE Communications Magazine* (2016-present), the *IEEE Trans. on Wireless Communications* (2012 present), the *IEEE Trans. on Molecular, Biological, and Multi-scale Comm.* (2015-present), the *IEEE Wireless Communications Letters* (2016-present), and the *IEEE/KICS Jour. of Comm. Networks* (2012-present).

**Fei Ji** (M'06) received the B.S. degree in applied electronic technologies from Northwestern Polytechnical University, Xian, China, and the M.S. degree in bioelectronics and Ph.D. degree in circuits and systems both from the South China University of Technology, Guangzhou, China, in 1992, 1995, and 1998, respectively.

She is currently a Professor with the School of Electronic and Information Engineering, South China University of Technology. She was the Registration Chair and the Technical Program Committee (TPC) member of IEEE 2008 International Conference on Communication System. Her research focuses on wireless communication systems and networking.